PMM/A-52

COMISION NACIONAL DE ENERGIA ATOMICA
DEPENDIENTE DE LA PRESIDENCIA DE LA NACION

SEXTO CURSO PANAMERICANO DE METALURGIA

Dentro del Programa Multinacional de Metalurgia
(Programa Regional de Ciencia y Tecnología - OEA)

TEORIA DE DISLOCACIONES

Dr. A. Smallman
(Dpto. de Metalurgia, Universidad de Birmingham)

Departamento de Metalurgia
Buenos Aires - Argentina
1970

PMM/A-52

COMISION NACIONAL DE ENERGIA ATOMICA
DEPENDIENTE DE LA PRESIDENCIA DE LA NACION

SEXTO CURSO PANAMERICANO DE METALURGIA

Dentro del Programa Multinacional de Metalurgia
(Programa Regional de Ciencia y Tecnología - OEA)

TEORIA DE DISLOCACIONES

Dr. A. Smallman
(Dpto. de Metalurgia, Universidad de Birmingham)

Departamento de Metalurgia
Buenos Aires - Argentina
1970

I. THEORETICAL STRENGTH OF CRYSTALS.

Once it was known that crystals are made up of a periodic array of atoms and that deformation takes place by slip, the magnitude of the shear stress required to produce plastic deformation could be determined easily. The theoretical strength of crystals was first calculated by Frenkel for a simple rectangular lattice Fig. 1. The shearing force

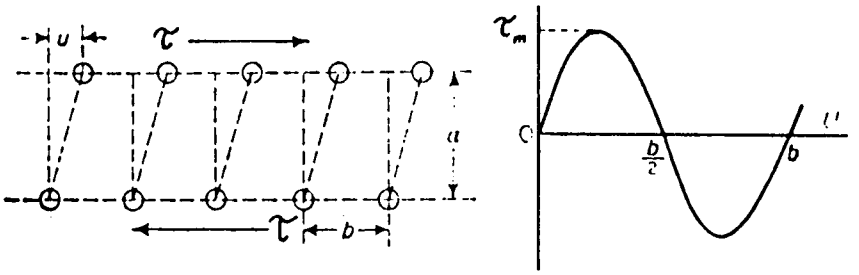

Fig. 1. Slip of a rectangular lattice.

required to move the top plane of atoms over the bottom plane will be periodic, since for displacements $u<b/2$ the lattice resists the applied stress but for $u<b/2$ the lattice forces assist the applied stress, and the simplest function with these properties is a sinusoidal relation of the form

$$\tau = \tau_m \sin (2\pi u/b) \simeq \tau_m 2\pi u/b \qquad 1.$$

where τ_m is the maximum stress at a displacement $u = b/4$, μ is the shear modulus, b the spacing of atoms in the shear direction. For small displacements the elastic strain given by u/a, where a is the spacing between the planes, is equal to τ/μ from Hooke's law, so that

$$\tau_m = \mu/2\pi \; b/a \qquad 2.$$

Since $b \approx a$, the theoretical strength of a perfect crystal is of the order of $\mu/10$. Refined calculations using a more realistic expression for the shearing force as a function of distance in the slip plane have shown that τ_m is $\sim \mu/30$. It is clear that perfect single crystals should be rather strong and difficult to deform, yet it is observed experimentally that annealed crystals are soft and easy to deform at very low stresses in the range $10^{-5}\ \mu - 10^{-4}\ \mu$, i.e. several orders of magnitude below the theoretical value.

2. THE CONCEPT OF A DISLOCATION.

This discrepancy of 10,000 or so between theory and experiment was satisfactorily explained, just before the last war, by three scientists working independently. Taylor, Orowan and Polanyi postulated that instead of a crystal shearing all the atoms in a given plane at the same time, the same end result was produced by shearing the crystal, a little bit at a time. There will of course be a disturbance of the lattice between the sheared and unsheared region of the crystal and it is the movement of these imperfections, or dislocations as they are now called, at low stresses that leads to plastic deformation.

In recent years it has been possible to produce crystals in the form of fibres with extremely small diameters. These crystals, called whiskers, are often free from dislocations and have withstood tensile stresses up to $\sim E/20$, where E is Young's modulus, without breaking or even yielding. Fig. 2 shows the tensile properties of a copper whisker, from which it is evident that such whiskers are strong when they are dislocation-free but that the strength vanishes as soon as slip and mobile dislocations are created.

A schematic three-dimensional diagram illustrating the propagation of a dislocation is given in Fig. 3 and it can be seen that when the slipped region has spread completely across the slip plane the top half of the crystal is displaced one atomic spacing b in the slip direction relative to the bottom half of the crystal. It can also be observed that the displacement is constant over the slipped area until it suddenly drops to zero at the dislocation line. The normal crystal structure, elastically strained of course, therefore exists everywhere but in the immediate vicinity of the dislocation line.

In general, the dislocation line makes an angle of between 0 and 90° with the displacement, or Burgers vector, b. However, the two extreme cases have been given special attention because any dislocation can be resolved into components at right angles, and also because such dislocations represent characteristic distortions of the crystal structure.

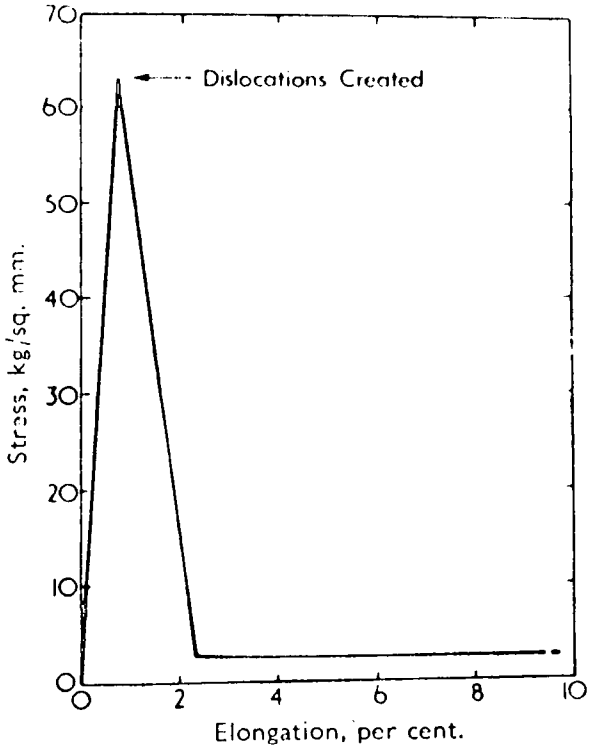

Fig. 2. Deformation curve of a dislocation-free copper crystal.

When the dislocation line lies perpendicular to its Burgers vector b it is called an edge dislocation, and when it lies parallel to b it is called a screw dislocation. The atomic structure of an edge dislocation is shown in Fig. 4

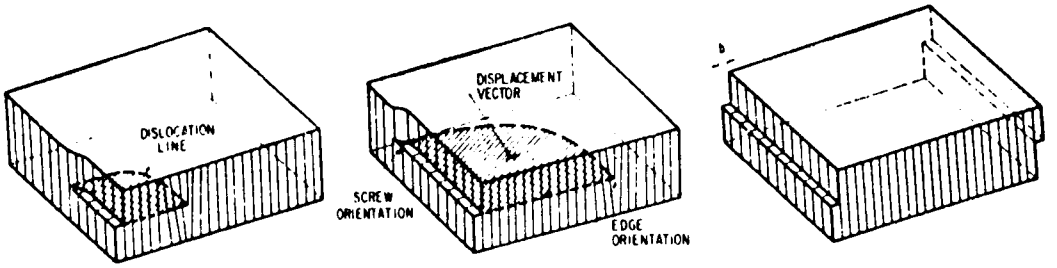

Fig. 3. Propagation of slip in a simple cubic structure.

where an extra half-plane of atoms is present above the slip plane. This half-plane was originally on the outside surface but has been pushed into the interior of the crystal. Most of the distortion is located near the edge of the extra half-plane, hence the name. When the extra half plane is above the slip plane it is called a positive edge dislocation and when it is below it is called a negative edge dislocation. Around a screw dislocation Fig. 5, the planes of atoms form a screw-like or helical

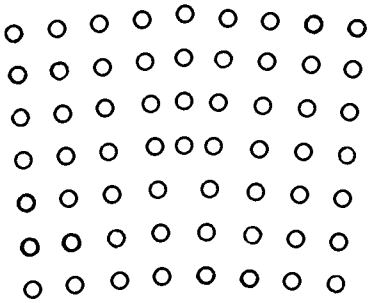

Fig. 4.

surface, and if the helix advances one plane when a clockwise path is taken along the screw axis, it is termed a right-hand screw; if the reverse is true, it is a left-hand screw.

An important property of a dislocation line is the value of the Burgers vector b. This is constant along the whole of the line and denotes the magnitude and direction of the displacement of the slipped portion of a crystal with respect to the unslipped part. A precise definition of the

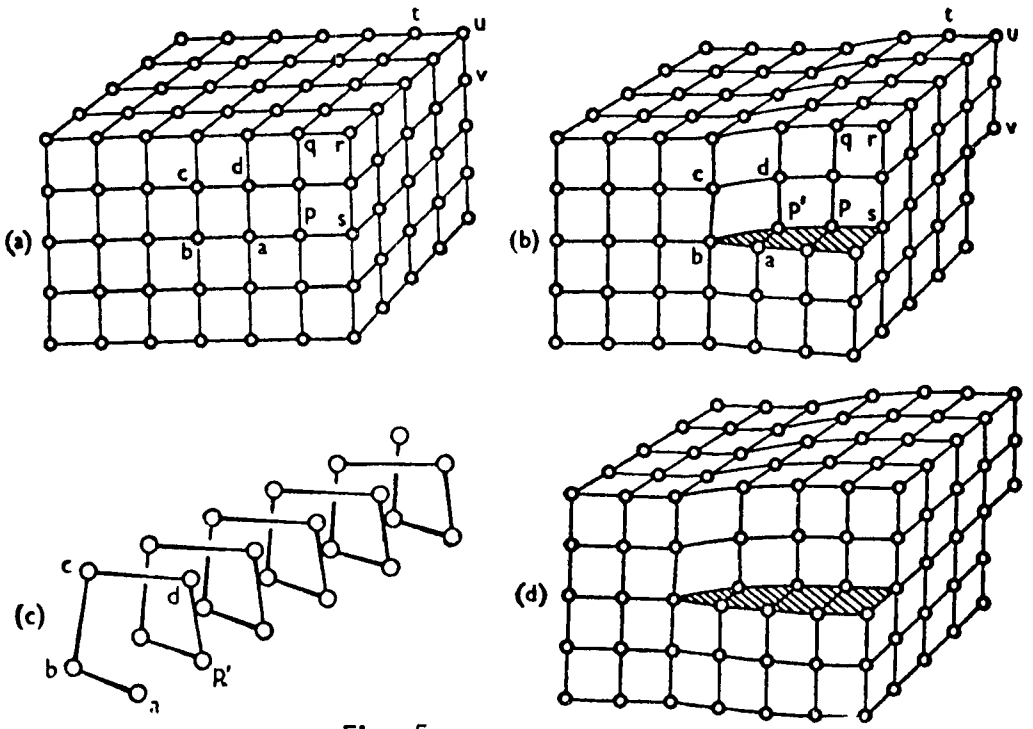

Fig. 5.

vector is obtained by comparing a Burgers circuit enclosing a dislocation with a crystallographically equivalent circuit in the perfect crystal. An equivalent definition is obtained if the circuit is first carried out in the perfect crystal. The closed circuit is shown in Fig. 6 (a) for a perfect crystal; the corresponding circuit for the imperfect crystal Fig 6 (b), following precisely the same sequence of lattice vectors, fails to close. The closure vector is the Burgers vector of the dislocation b and indicates

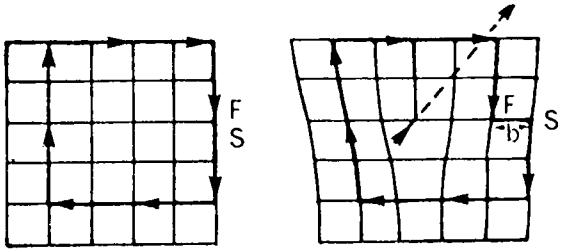

(a) (b)

Fig. 6. Burgers circuit.

the magnitude and direction of displacement of the crystal by the movement of the dislocation. However, it is clear that the definition depends on the direction of the circuit; if the direction of the circuit is reversed, the sense of the closure vector and hence b is also reversed. It is therefore necessary to choose one direction along the dislocation line as positive. The most common convention is that represented by $\overrightarrow{FS/RH}$ and describes the situation for a Burgers circuit taken in the right-hand sense first around the dislocation, when the Burgers vector connects the finish of the circuit (F) to the start (S) in the perfect crystal. DeWit* has summarized the use of the different conventions.

It is usual to express the Burgers vector of a dislocation in a particular crystal structure in terms of cell co-ordinates. For the f.c.c. lattice, for example, a unit dislocation produces shear displacement equivalent to that from a cube corner to a face centre, and the vector that describes it has components $a/2$, $a/2$, 0, where a is the lattice parameter. This may be written $a/2$ [110], from which the slip direction [110] and strength of the dislocation, i.e. $|b| = \sqrt{a^2/4\,(1+1+0)} = a/\sqrt{2}$, is easily obtained.

4. DISLOCATION GLIDE AND CLIMB

When a dislocation moves across a slip plane, as shown in Fig. 3 it will be noticed that the same shear displacement equal to the Burgers vector b is produced by positive and negative edge dislocations moving in opposite directions, and screw dislocations moving at right angles to the edge dislocations. A basic feature of slip by the propagation of dislocations is that the slip plane is defined by the plane containing both the line of the dislocation and its Burgers vector b. This feature gives rise to an important difference between the motion of an edge and that of a screw. The edge dislocation is restricted to glide in one slip plane only,

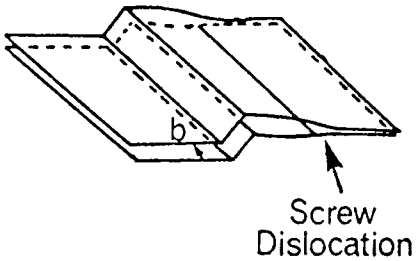

Fig. 7. Cross-slip of a screw dislocation.

* *R. de Wit, Acta Met., 1965, 13, 1210.*

whereas the screw dislocation having its line parallel to the Burgers vector can, in principle, move on any lattice plane traced by the screw axis on which there is a sufficient shear stress. In general, however, the screw dislocations move in certain crystallographic planes, e.g. (111) planes in f.c.c. metals, but unlike edge dislocations the screws can glide out of the original slip plane and move on another having a slip direction in common with the original plane. This process, illustrated in Fig. 7 is known as cross-slip.

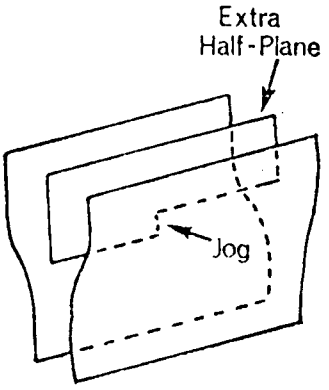

Fig. 8. Dislocation climb.

Although the edge dislocation is restricted to moving conservatively in one plane defined by the line and the Burgers vector (with the density of material in the plane conserved during the motion), it can move non-conservatively by climb in a direction normal to the slip plane, as shown in Fig. 8. The extra half-plane of atoms of the edge dislocation can be made to lengthen or shorten by adding atoms to or removing atoms from the edge of the half-plane. This can occur if atoms migrate from lattice sites near the dislocation into sites on the edge of the half-plane, so that the dislocation climbs down; it follows that vacant sites are created in the lattice away from the dislocation. Conversely, vacancies can migrate to the edge of the half-plane causing it to climb up as they are annihilated. The dislocation can therefore act as either a source or a sink for vacancies. In practice, the vacancies will not arrive at the dislocation at the same instant or uniformly and hence the edge of the half-plane of atoms will not lie in a

particular slip plane; instead some sections will lie in one plane and other sections in parallel neighbouring planes. The short length of dislocation not lying in the same slip plane as the main dislocation but having the same Burgers vector is called a jog.

5. CONSERVATIVE AND NON-CONSERVATIVE MOTION

The process of climb requires the movement of atoms to or from the dislocation line. Such non-conservative motion of an edge dislocation is common at elevated temperatures where there is a high concentration of vacancies and sufficient thermal activation for diffusion. Climb therefore plays an important role in the softening of crystals hardened by deformation, quenching, or irradiation, as discussed in Section 10. It is possible, however, for jogs to be produced at temperatures too low for appreciable diffusion and for edge dislocations to move non conservatively. This happens when jogs are formed on gliding dislocations.

With increasing plastic deformation, slip occurs on more than one slip system, e.g. in f.c.c. metals more than one type of (111) plane operates, and since the slip planes of the primary system intersect the slip planes of the secondary system, gliding dislocations may have to intersect dislocations crossing the slip plane on another system. Any dislocation threading the primary slip plane is called a forest dislocation. Two examples will suffice to illustrate the geometry of jogs formed in this way. Fig. 9 shows the intersection of edge dislocations having Burgers vectors at right angles to each other. The dislocation AB is increased in length by $|b|$ the magnitude of the Burgers vector of the dislocation intersecting it. No jog is formed in the dislocation XY because the Burgers vector AB is parallel to the line of the dislocation XY. If the two intersecting dislocations have parallel Burgers vectors, then a jog is produced in each dislocation equal in length to the magnitude of the Burgers vector of the other. Fig. 10. shows a particularly important example of intersecting dislocations, because one of them is a screw dislocation and all the jogs produced are edge in character.

Jogs in pure edge dislocations do not affect the glide of the main dislocation line. An examination of Fig. 9 shows that the jog PP' is a piece of edge dislocation that can readily move conservatively in the plane in which the jog lies. However, as can be seen in Fig. 31 a jog in a screw

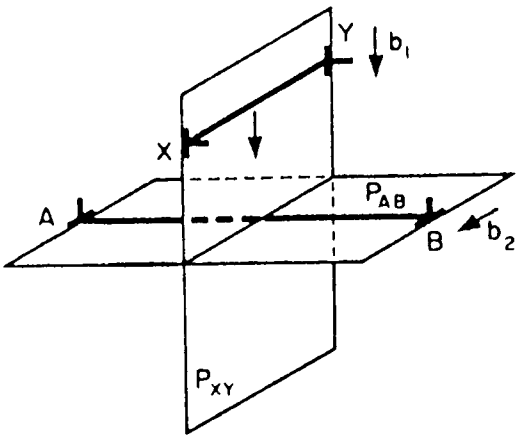

(a)

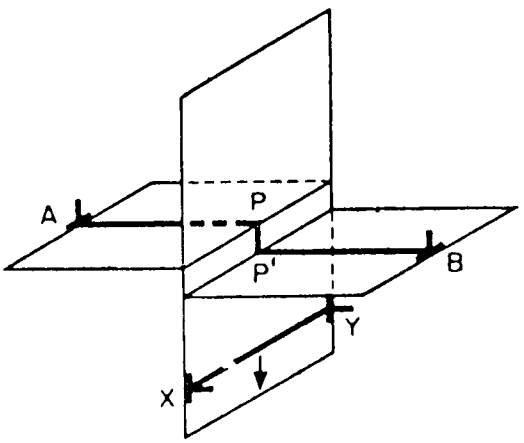

(b)

[*Courtesy McGraw-Hill.*

Fig. 9 Jog formation by intersecting edge dislocations. (*After Read.*)

dislocation is an edge dislocation and, since this glides in the plane containing its line and Burgers vector, the only way it can move conservatively is along the screw-dislocation axis. If the screw dislocation glides forward taking the jog with it, then the jog is forced to climb since it moves perpendicular to its Burgers vector. As pointed out in the previous section, this is a non-conservative process involving the formation of either vacancies or

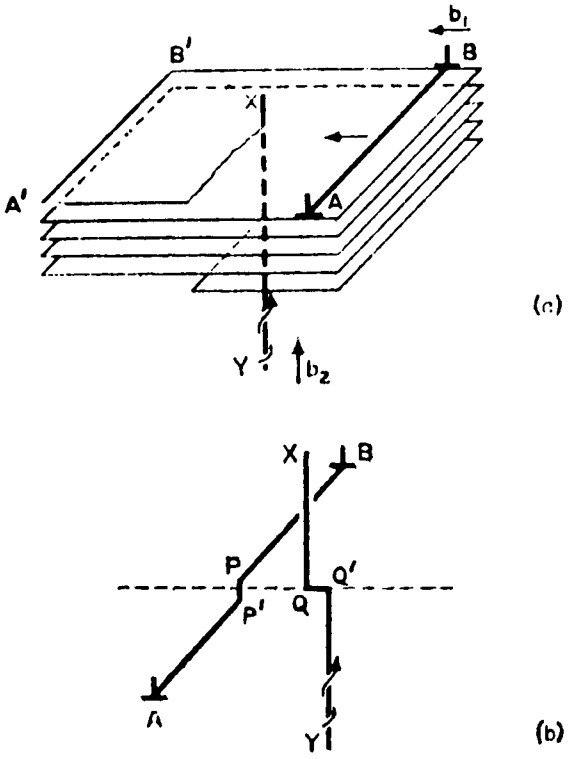

[*Courtesy McGraw-Hill.*

Fig. 10 Jog formation by intersecting screw dislocations. (*After Read.*)

interstitials depending on which way the jog is forced to climb. A jog that moves in such a direction that it produces vacancies is called a vacancy jog; if it moves in the opposite direction it is an interstitial jog. This is one way in which point defects are produced during plastic deformation.

So far we have considered only elementary jogs or those with a height equal to one atomic plane spacing, but it is possible to have composite jogs where the jog

height is several atomic plane spacings. Such jogs can be produced, for example, by part of a screw dislocation cross-slipping from the primary plane to the cross-slip plane, as shown in Fig. 11.

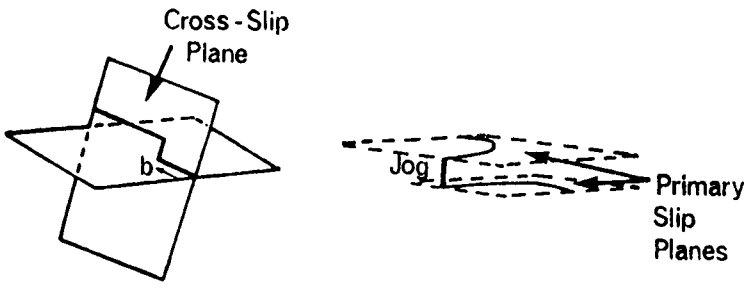

(a) (b)

Fig. 11. Formation of: (*a*) a multiple jog; (*b*) a dislocation dipole.

In this case, as the screw dislocation glides forward it trails the composite jog behind, since this cannot glide in the forward direction. As a result, two parallel dislocations of opposite sign are created in the wake of the moving screw, as shown in Fig. 11, this arrangement is called a dislocation dipole. Dipoles formed as debris behind moving dislocations are frequently seen in electron micrographs taken from deformed crystals and an example is shown in Fig 36.

6. ELASTICITY PROPERTIES OF A DISLOCATION

To calculate the energy associated with, and the distortion surrounding, a dislocation it is usual to consider the dislocation as contained in a continuous medium that is everywhere elastic and isotropic. It then follows that the stress and displacements field derived on this assumption will be valid only for small

strains and will break down at the centre of the dislocation where the strains are large. Hence it is necessary to define a core to the dislocation at cut-off radius $r_0 (\sim b)$ inside which elasticity theory is no longer applicable.

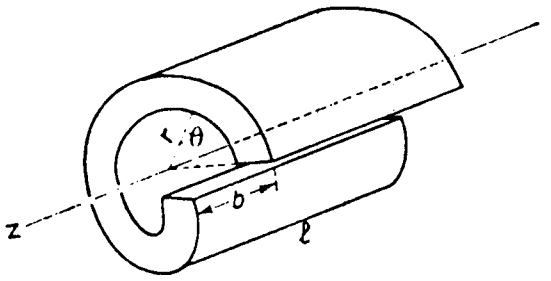

Fig. Continuum model of a screw dislocation.

A screw dislocation can therefore be considered Fig. 12 as a cylindrical shell of length ℓ and radius r. A discontinuity of displacement exists only in the z-direction, i.e. parallel to the dislocation, and defines anti-plane strain such that the displacement in the $x - y$ plane is $u = v = 0$, and that in the z-direction is $w = b$. The elastic strain thus has to accommodate a displacement $w = b$ around a length $2\pi r$. In an elastically isotropic crystal the accommodation must occur equally all around the shell and indicates the simple relation

$$w = [b/2\pi] \tan^{-1} [y/x] = b\theta/2\pi$$

in cartesian (x, y, z) and polar (r, θ, z) co-ordinates, respectively. The corresponding (shear) strain $\gamma_{\theta z} = (\gamma_{z\theta}) = b/2\pi r$ and shear stress $\tau_{\theta z} (= \tau_{z\theta}) = \mu b/2\pi r$, which acts on the end faces of the cylinder, with σ_{rr} and $\tau_{z\theta}$ equal to zero.

Alternatively, the stresses are given by

$$\left.\begin{aligned} \tau_{xz}\,(=\tau_{zx}) &= -\mu b/2\pi\left[y/(x^2+y^2)\right] \\ \tau_{yz}\,(=\tau_{zy}) &= \mu b/2\pi\left[x/(x^2+y^2)\right] \end{aligned}\right\} \qquad 3.$$

all other stresses being zero. The field of a screw dislocation is therefore purely one of shear, having radial symmetry with no dependence on θ. This mathematical description is related to the structure of a screw which has no extra half-plane of atoms and cannot be identified with a particular slip plane.

An edge dislocation has a more complicated stress and strain field than a screw. The distortion associated with the edge dislocation is one of plane strain, since there are no displacements along the z-axis, i.e. $w = 0$. In plane deformation the only stresses to be determined are the normal stresses σ_{xx}, σ_{yy} along the x and y axis, respectively,* and the shear stress τ_{xy} which acts in the direction of the y-axis on planes perpendicular to the x-axis. The third, normal stress $\sigma_z = \nu(\sigma_x+\sigma_y)$, where ν is Poisson's ratio,+ and the other shear stresses τ_{yz} and τ_{zx} are zero. In polar co-ordinates r, θ, and z, the stresses are σ_r, σ_θ, and $\tau_{r\theta}$.

Even in the case of an edge dislocation the displacement b has to be accommodated around a ring of length $2\pi r$, so that the strains and the stresses must contain a term $B/2\pi r$. Moreover, because the atoms in the region $0 < \theta < \pi$ are under compression and those in the region $\pi < \theta < 2\pi$ are in tension, the strain field must be of the form $(b/2\pi r)f(\theta)$, where $f(\theta)$ is a function such as $\sin\theta$ that changes sign when θ changes from 0 to 2π. It can be shown, in fact, that the field is described by the stress function

$$\psi = -Dr\ln r\sin\theta = -Dy\ln(x^2+y^2)^{\frac{1}{2}}$$

where $D = \mu b/2\pi(1-\nu)$ and the stresses are given by

$$\sigma_r = \sigma_\theta = -(D\sin\theta)/r;\quad \tau_{r\theta} = (D\cos\theta)/r \qquad 4.$$

* *Because different symbols are used for normal and shear stresses, the second suffix in the notation for normal stress can be dropped without loss of clarity and the normal stresses written* σ_x, σ_y, σ_z.

+ *Defined in a normal tensile test as the ratio of the strain in the transverse direction to that in the axial direction.*

in polar co-ordinates, and

$$\sigma x = -D\frac{y(3x^2 + y^2)}{(x^2 + y^2)^2} \quad \sigma y = D\frac{y(x^2 - y^2)}{(x^2 + y^2)} \quad \tau xy = D\frac{x(x^2 - y^2)}{(x^2 + y^2)} \qquad 5.$$

in cartesian co-ordinates.

The above equations show that the stresses around dislocations fall off as $1/r$ and hence the stress field is long-range in nature. Dislocations therefore strongly interact with each other elastically. For a screw dislocation the stress field has radial symmetry and consequently the forces between parallel screw dislocations are central forces. In the case of edge dislocations the forces are not central forces.

From the known elastic properties it is possible to calculate the energy associated with a dislocation line. The elastic strain energy of a screw dislocation can be obtained by taking the strain energy in an annular ring around the dislocation of radius r and thickness dr to be $(1/2)$, $\mu\,(b/2\pi r)^2 . 2\pi r . dr$. The total strain energy per unit length of dislocation is then obtained by integrating from r_0, the core radius, to r, the outer radius of the stress field, and is

$$E = (\mu b^2/4\pi)) \int_{r_0}^{r} dr/r = (\mu b^2/4\pi)\left\{\ln\left[r/r_0\right]\right\} \qquad 6.$$

With and edge dislocation this energy is modified by the term $(1 - \nu)$ and hence is ~50% greater than a screw. For a unit dislocation in a typical crystal $r_0 \sim 3 \times 10^{-8}$ cm, $r \sim 3 \times 10^{-4}$ cm, $\ln [r/r_0] \simeq 9.2$, so that the energy of a dislocation is approximately μb^2 per unit length or $\mu b^2 \sim 5$ eV per atom place threaded by the dislocation. To this value must of course be added the energy of the core of the dislocation, which has been estimated to be $\sim \frac{1}{2} - 1$ eV per atom length.

Equation 6 shows that the energy of a dislocation depends on b^2, and hence dislocations with the smallest b are energetically favoured, which accounts for the slip directions found in common crystal structures. From strain-energy considerations it is also readily seen that two dislocations of opposite sign (+b and -b) on the same slip plane reduce their energy to zero when they move together and annihilate each other; there is therefore a force of attraction between them that relieves the strain energy of the lattice. Conversely, two dislocations of the same sign will repel each other, because the strain energy of two dislocations on moving apart would be

$2 \times b^2$, whereas if they combined to form one dislocation of Burgers vector 2b, the strain energy would then be $(2b)^2 = 4b^2$; a force of repulsion thus exists between them. The force is, by definition, equal to change in energy with position and for screw dislocations is simply $F = \mu b^2/2\pi r$, where r is the distance between the two dislocations. Since the stress fields around the screw dislocations have cylindrical symmetry the force of interaction depends only on the distance apart, and the above expression for F applies equally well to parallel screw dislocations on neighbouring slip planes.

The forces between parallel edge dislocations are complicated by the angular-dependence of the stress field. In addition to the force F directed along the line joining their centres (the central force that follows the strain-energy arguments given above), there is also a force tending to alter the θ co-ordinate of one dislocation relative to the other. Thus, edge dislocations of the same sign on neighbouring slip planes will tend to align themselves one above the other, so that the expanded region beneath the one dislocation somewhat compensates the compressed region above the other dislocation Fig. 13. Such an arrangement of dislocations constitutes a small angle boundary, since a wall of dislocations is the easiest way to join together two crystals with small misorientations, as shown in Fig. 13. By this arrangement the long-range stresses from the individual dislocations are cancelled out beyond a distance of the order of h from the boundary, where h is the dislocation separation in the boundary.

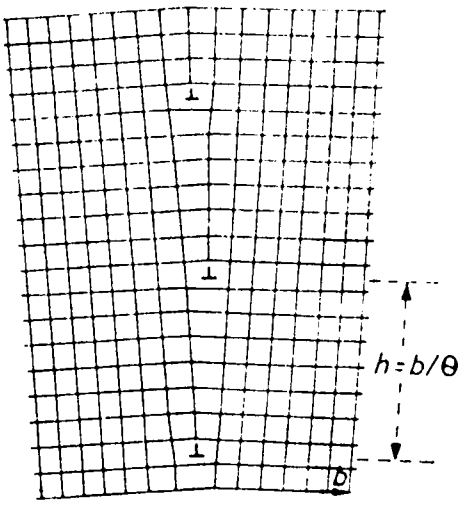

Fig. 13.. Small-angle boundary.

Clearly, two edge dislocations of opposite sign will not want to line up above each other, and in equilibrium they will take up a position at 45° to each other. All these processes lower the strain energy of the lattice, some leading to a reduction in dislocation density, and consequently are mechanisms that operate during recovery after deformation. The process of alignment of dislocations in walls is particularly important in the annealing of severely deformed crystals, and is known as polygonization.

The presence of point singularities in the lattice, i.e. solute atoms, interstitials, and vacancies, also gives rise to elastic stresses that can interact with the stress field around a dislocation. The simplest form of this interaction is due to the size-effect, in which a solute atom of radius $r = r_0(1 + \epsilon)$ is considered to sit in a hole of radius r_0 in an elastically isotropic medium. For a misfit parameter $\epsilon > 0$ the atom will produce a symmetrical distortion of the surrounding matrix either positive or negative, depending on whether it is bigger or smaller than r_0, and will interact with the hydrostatic component of the stress field around a dislocation. The interaction energy is the work done against the local stress field in producing the distortion and is given by

$$E_I = p\Delta V \qquad 7.$$

where $\Delta V = 4\pi\epsilon r_0^3$ is the volume change associated with the solute atom. For an edge dislocation p is given by the stress equations previously derived, and hence for an atom situated at a point $(R\theta)$ in the field of a positive edge dislocation gives

$$E_I = (4/3)\{(1 + \nu)/(1 - \nu)\}\mu b\epsilon r_0^3 \left[\sin\theta/R\right] \qquad 8.$$

The maximum value of E_I reached when $R = r_0 \sim b$, $\nu = 1/3$, and $\sin\theta = 1$, is $E_I \simeq 8\epsilon\mu b^3/3$; with $\epsilon \simeq 0.05$ and $\mu b^3 = 4$ eV, the interaction energy is $\sim \frac{1}{2}$ eV.

To a first approximation the atom does not interact with a screw dislocation since there is no dilation around the screw. However, a second-order dilation exists around a screw* that gives rise to a non-zero interaction falling off with

*H. Pleiderer, A. Seeger, and E. Kroner, Z. Naturforsch, 1960 [A], 15, 758.

distance from the dislocation according to $1/r^2$. In real crystals, however, anisotropic elasticity will lead to first-order size-effects even with screw dislocations and hence a substantial interaction is to be expected. A second, different, type of elastic interaction can exist which arises from the fact that the elastic constants of the solute atom differ from those of the solvent atom. Such an inhomogeneity interaction has been analysed[+‡] both for rigid and soft spherical regions; the former corresponds to a relatively hard impurity atom and the latter to a vacant lattice site. It is generally believed that the inhomogeneity effect dominates the size effect for vacancy/dislocation interactions.

7. ORIGIN OF DISLOCATIONS

From the previous discussion it is clear that most materials contain dislocations. A dislocation density of 10^6 cm of dislocation line per cm^3 is typical of soft well-annealed metal crystals and 10^{11} - 10^{12} cm/cm^3 for heavily deformed crystals. The mechanisms whereby the density increases from 10^6 to 10^{12} cm/cm^3 during deformation will be dealt with later, but here we consider the origin of dislocations and not their multiplication.

It might be thought that dislocations, like vacancies, are crystal defects having a finite thermodynamic equilibrium concentration at a given temperature above 0°K. However, it is readily shown that the dislocation is thermodynamically unstable and should anneal out. This instability stems from the fact that the large distortion associated with the dislocation gives rise to a
+ lattice strain energy that raises the internal energy of the crystal by $\sim 10^8$ eV per cm length. Entropy changes in the crystal are negligible compared with this large strain energy and hence, although geometrically feasible, dislocations exist as thermodynamically unstable lattice defects.

This behaviour contrasts with that of a vacancy, which can exist in appreciable concentrations in thermodynamic equilibrium. If the energy of vacancy formation is E_f the number n of vacancies among N crystal sites is given by

$$n = AN \exp\left[-Ef/kT\right]$$

or the fractional concentration

+ *R. Bullough and R.C. Newman, Phil. Mag., 1962, 7, 529.*

‡ *R. Bullough and R.C. Newman. J. Phys. Soc. Japan, 1963, 18, Suppl. III, 27.*

$$c = n/N = A \exp\left[-E_f/kT\right] \qquad 9.$$

where A is a vibrational entropy term usually taken to be close to unity. For most metals $Ef \lesssim$ leV, as shown in Table I and hence just below the melting point T_m, about one site in 10^4 is vacant. This means that in a crystal 1 cm^3 in size with $\sim 10^{22}$ atom sites, there will be 10^{18} lattice vacancies at temperatures close to T_m. It also follows from equation 9 that

Table I. Values (eV) of Energies Required to Form (Ef) and Move (E^m) Vacancies in Some Metals and Alloys, together with the Self-Diffusion Energy (E_D)

	Ag	Au	Cu	Al	Ni	Mg	Fe	Mo	W	AuZn	NiAl
E_f	1.03	0.98	1.0-1.1	0.76	1.4	0.9	2.13	2.4	3.3	0.43	1.05
E_m	0.88	0.82	1.0-1.1	0.62	1.5	0.5	0.76	1.3	1.9	0.47	2.4
E_D	1.91	1.81	2.0-2.2	1.38	2.9	1.4	2.9	3.7	5.2	0.9	3.4

$n < 1$ for E_f 50 T_m or ~4eV per atom for aluminium; hence only defects with a small value of E_f can exist in significant numbers in thermal equilibrium at a given temperature. This estimate also shows that interstitial-type point defects, for which $E_f \simeq$ 4eV (since a high strain energy is required to push the neighbouring atoms apart in order to lodge an atom in an interstitial site), usually occur in very low concentrations in crystals, even at high temperatures. Such defects, unlike vacancies, are thus unimportant in solid-state reactions. Interstitials in excess of the equilibrium concentration may be formed, however, by bombarding the metal with high-energy irradiation such as neutrons or α-particles. The fast-moving particles occasionally collide with the atoms of the structure knocking them off their lattice site, so that eventually they become lodged in an interstitial site.

Crystal Growth

A dislocation is a geometrically feasible defect, and although thermodynamically unstable, is essential to certain processes of crystal growth and chemical catalysis on crystal faces. From Fig. 14 for example, it can be seen that a crystal containing a screw dislocation that emerges on a suitable external face has a ledge or step which provides sites for centres of chemical activity on the face. It is possible for atoms to be deposited on or evaporated from such ledges without destroying the usefulness of the site, but with increasing distance from the point of emergence of the dislocations more atoms have to be added to make a complete revolution and this leads to the formation of a growth spiral, as shown in Fig. 15, the rate of growth of crystals is therefore increased and hence the growth of crystals is favoured by the presence of dislocations.

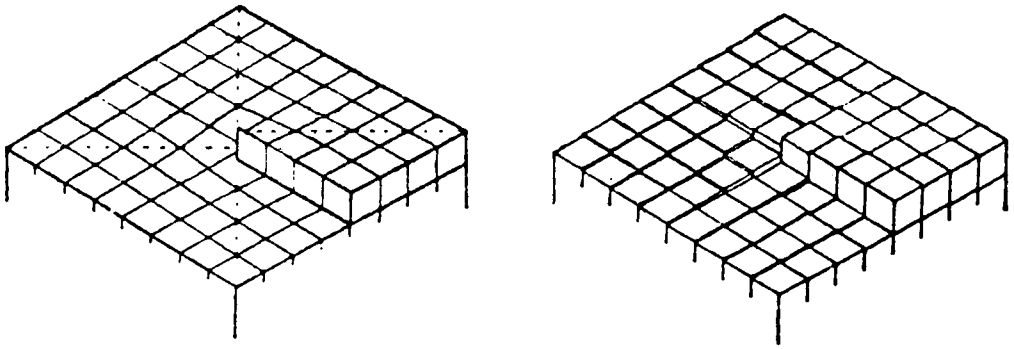

(*a*) (*b*)

[*Courtesy Faraday Society.*

Fig. 14. The end of a screw dislocation. (*After Frank.*)

Non-Equilibrium Cooling

By cooling a crystal very rapidly from a temperature somewhat below its melting point, e.g. by quenching a metal into water, it is possible to retain the high concentration of vacancies that exists in thermodynamic equilibrium at the high temperature in supersaturated solution. On ageing at room or slightly elevated temperature, the concentration of vacancies above the equilibrium concentration ($\sim 10^{-14}$) at room temperature, diffuse about inside the crystal. Some of the vacancies

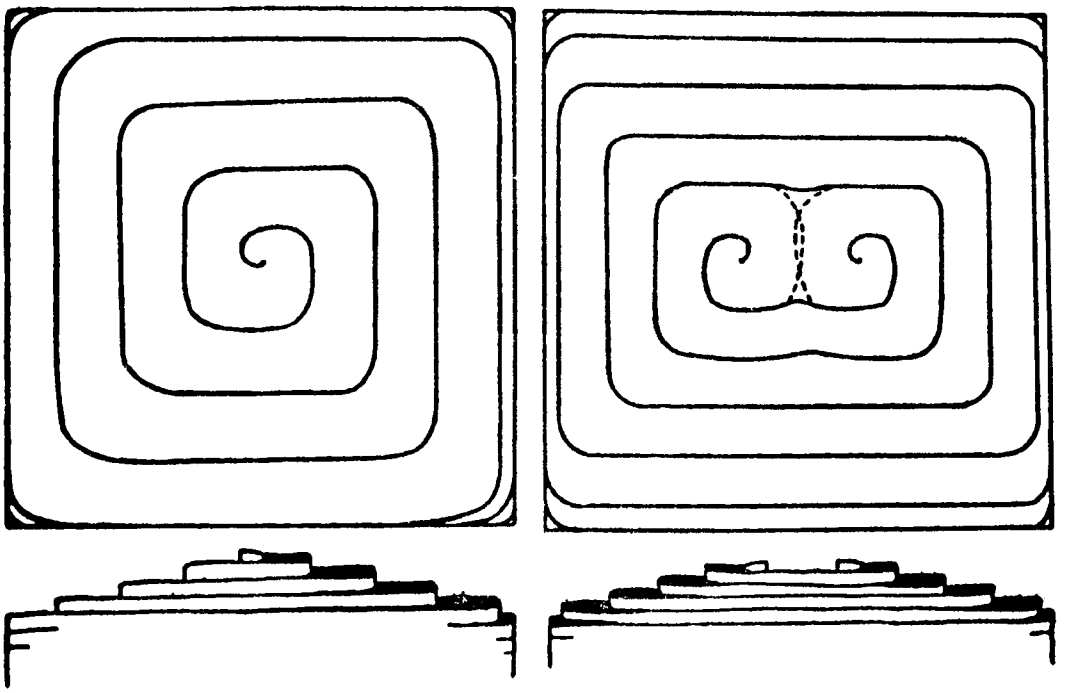

[*Courtesy Royal Society.*

Fig.15 **Growth pyramid due to a single screw dislocation.**
(*After Burton, Cabrera, and Frank.*)

escape to the surface of the crystal (grain boundary of a polycrystal) and are lost, some are annihilated at dislocations thereby producing climb, and others group into clusters. These changes can be detected by studying the changes in physical properties, such as length and electrical resistivity, as a function of ageing time, and from the kinetics of the process important parameters can be obtained section 9.

All these processes reduce the excess point-defect concentration, but the most efficient method is to precipitate the vacancies to form a large

void within the crystal. Planar aggregates one atomic layer in thickness are commonly formed, and as these aggregates grow the disc-shaped void eventually becomes unstable and collapses. The process gives rise to a prismatic dislocation loop, as shown in Fig. 16. The Burgers vector of this dislocation lies perpendicular to the plane of the loop and is equal in magnitude to the spacing of the lattice planes on which it lies. The dislocation loop can continue to grow by climb as a result of the addition of more and more vacancies to jogs on the dislocation line. It is readily shown that a vacancy concentration σ, $\sim 10^{-4}$ would give $\sim 10^{14}$ loops of 300 Å dia. per cm^3. This creates $\sim 10^{10}$ cm/cm^3 of dislocation line; hence with more moderate, but non-equilibrium, cooling, such as would occur in casting, it is not unreasonable to create $\sim 10^{6}$ cm/cm^3. The vacancies usually aggregate on to the close-packed (111) planes of the f.c.c. structure, the stacking sequence is then changed from ABCABCABC to ABCA↓BABCA where the arrow indicates the position of the stacking fault. It is therefore evident that the dislocation loop encloses an area of stacking fault that has associated with it an extra energy γ ($ergs/cm^2$) known as the stacking-fault energy.

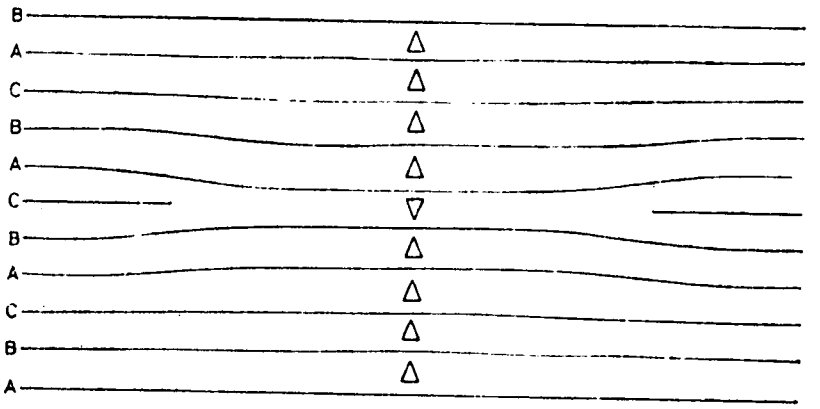

Fig. 16. Frank sessile dislocation.

Mechanical and Thermal Stress

The creation of a dislocation in a region of a crystal that is perfect clearly involves slip over part of the slip plane in that crystal. For such homogeneous nucleation of dislocation the theoretical shear strength of a perfect lattice must be reached which, as we have seen is $\sim \mu/30$. Since the energy of a dislocation is several electron volts per atomic plane threaded by the dislocation, thermal activation cannot help in the nucleation process. The probability of a thermal fluctuation of energy E, taking place is $\exp[-E/kT]$ and hence, since $kT \sim 1/40$ eV at room temperature, thermal activation would not reasonably provide >2-3 eV; this energy is much less than that of a small dislocation loop a few atom spacings in diameter. Moreover, even if such a loop could be established by some rare statistical event, it would require an applied stress close to the theoretical shear stress to expand.

Although the applied stress is well below the theoretical shear stress, it is nevertheless possible to raise the stress to this level in local regions of the crystal. For example, thermal stresses sufficient to create dislocations may be set up in cooling materials that are poor heat conductors if a temperature gradient of 10^4 degC/cm is produced in a material with a coefficient of thermal expansion of $\sim 10^{-5}$/degC. Stress concentrations can also arise at impurity atoms and precipitated particles of sufficient magnitude to necleate dislocations heterogeneously. A particularly striking demonstration of this is the prismatic punching of dislocation loops from inclusions as a result of the stresses produced by differential expansion or volume change in a precipitate during cooling. These stresses can be relieved by the generation of prismatic dislocation loops at the precipitate, which propagate out along a glide cylinder from the precipitate. The stresses in the vicinity of a precipitate are most likely to be compressive; hence, to relieve the stress requires the movement of material outward away from the surface adjacent to the inclusions. In this case the loops generated would be equivalent to platelets of interstitial atoms. Conversely, if the inclusion contracts more than the matrix, a series of prismatic loops equivalent to vacancy platelets would be punched out. The first experiments to demonstrate this punching effect were performed by Jones and Mitchell,* who embedded glass spheres in specimens of silver chloride, but many examples of punched-out dislocations have since been observed using thin-film transmission electron microscopy.

In real materials other stress concentrations such as cracks, twins, surface flaws, &c., are also capable of nucleating dislocations.

*D.A. Jones and J.W. Mitchell, Phil. Mag. 1958, 3, 1.

8. OBSERVATIONS OF CRYSTAL IMPERFECTIONS.

In recent years many methods have been developed for observing dislocations, stacking faults, and even point defects in crystals; these include etch-pitting, decoration with impurity atoms and precipitates, and microscopy methods involving either, X-rays, or gas ions.

Etch Pitting.

Etching techniques reveal dislocations Fig. 17 by producing sharp pits at the points at which dislocations emerge from the surface of crystals. The direct correspondence between a dislocation core and an etch-pit was proved initially by etching surfaces exhibiting growth spirals, and later by Vogel et al.,[+] who showed that the spacing (h) of pits in a low-angle tilt boundary of known tilt angle (θ) was in agreement with that predicted for the spacing of dislocations ($h = b/\theta$) from dislocation theory, section 6.

The mechanism governing the formation of an etch-pit at a dislocation is not completely understood. Impurities segregated to dislocation have an important effect on the etching behaviour and are probably essential for the initiation of the pit, but "clean" dislocations created by deformation can be etched, indicating that impurities, at least in the crystal, are not essential and that the important parameter is the local lattice strain energy associated with the dislocation. Impurity ions in the etching reagent are however essential to pit formation, and, since the pit must deepen faster than it widens, a likely mechanism involves the absorption of impurities on the sides of the pit to poison the surface steps and slow down the rate of dissolution there.

A difficulty associated with the etch-pit technique is to ensure that pits do in fact correspond with the points of dislocation emergence. If the density of dislocations is high, it is possible that only one etch-pit will show up at a closely associated group of dislocations because of the limitations of local resolution. It is also possible that impurity clusters and not dislocations will give rise to pits. However, within these limitations the method is very useful for the

[+] *F.L. Vogel, W.G. Pfann, H.E. Corey and E.F. Thomas, Phys. Rev. 1953, 90, 489.*

determination of dislocation densities and distribution in materials with low dislocation contents, i.e. $< 10^6/cm^2$, by etching successive sections through the crystal. The movement of dislocations can also be followed by repeated etching of a crystal after successive straining. The site of a dislocation at rest in a crystal appears as a sharp-bottomed pit, as shown in Fig. 17 but if the dislocation is moved by application of a stress and the specimen etched again, the new site of the dislocation is shown up sharply, while the old pit from which the dislocation has moved develops into a flat-bottomed pit. Since the etch-pit does not pin the dislocation, the technique has been used extensively for the measurement of dislocation velocity v and its dependence on stress and temperature section 10 where v is the distance moved by dislocation divided by the duration of the stress pulse.

Decoration Technique

The fact that there is an elastic interaction between the strain field of a dislocation and that surrounding a solute atom or precipitate is utilized in the decoration technique for revealing dislocations. The decoration process is usually effected by heat-treating the specimen to enable a second phase to precipitate preferentially on the dislocations. In metallurgy, precipitation-hardening alloys have been examined, the precipitate revealing dislocations on the metal surface, but in general, most of the work has been carried out on optically transparent crystals.

The technique has proved particularly useful in studying silicon, where the decoration is produced by diffusing copper into the silicon crystal at 900°C so that on cooling to room temperature the copper precipitates on dislocations. When the silicon crystal is examined optically by infrared radiation, the dislocation-free areas transmit the infra-red light but dislocations decorated with copper are opaque. The first observations of dislocations employed decoration by means of particles of photolytic silver in transparent crystals of silver bromide and chloride. In this case, the silver decoration occurs simply as a result of exposure to light and no heating is required, thus eliminating the main disadvantage of the technique, which is the modification of the dislocation arrangement during heat-treatment.

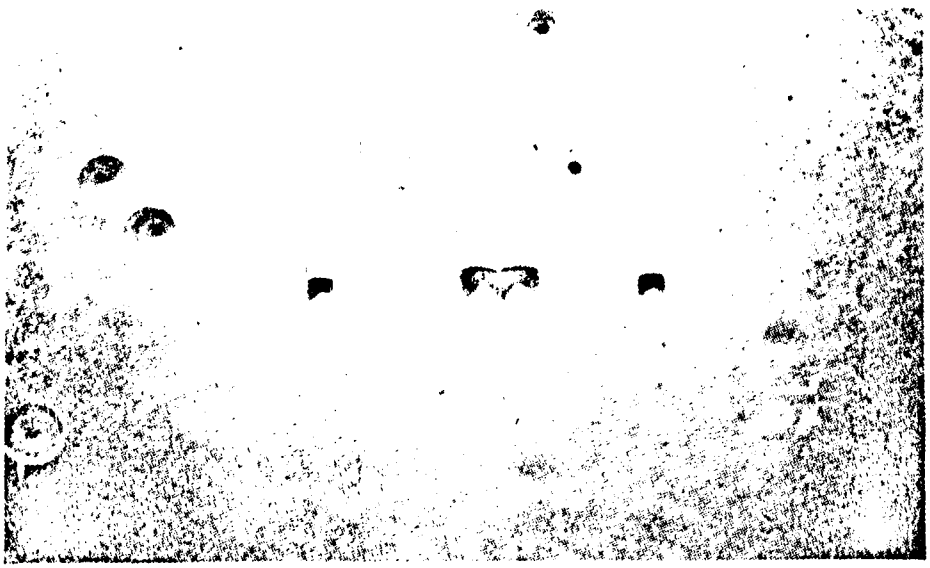

(*a*)

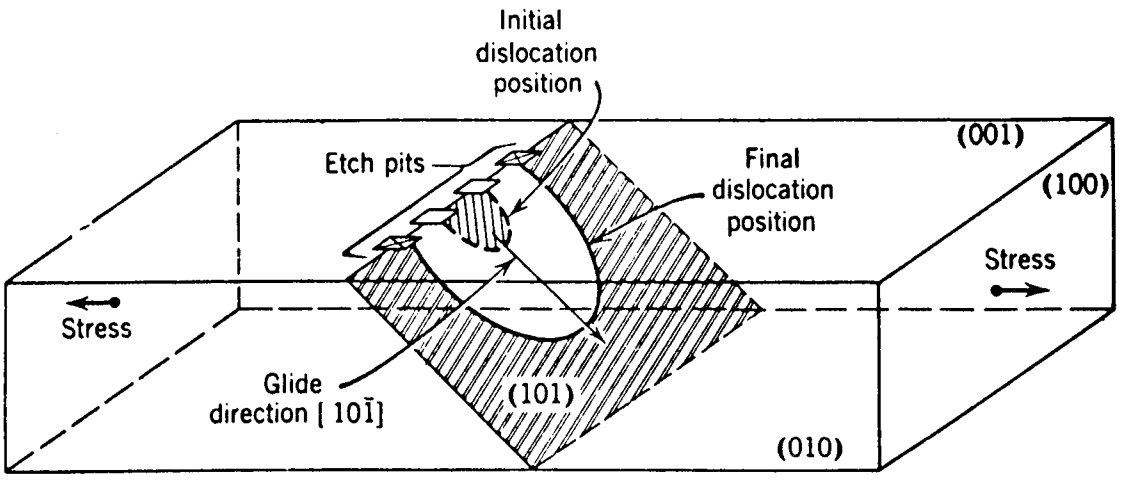

(*b*)

Fig. 17. Etch-pits showing motion of an individual dislocation loop in a lithium fluoride crystal. (*After Gilman.*)

Electron Microscopy

Electron microscopy has now become a well-established technique for studying defects in crystals. Essentially, this involves the preparation of thin crystal sections of the order of 3000 Å thick and examining them in transmission in the electron microscope operating at 100 kV. Various methods have been developed to obtain specimens sufficiently thin to transmit electrons; these include: (i) producing thin sections (~0.001 in.) by either rolling, spark erosion, diamond sawing, or ultrasonic cutting, suitable for final thinning by chemical or electrolytic polishing, and

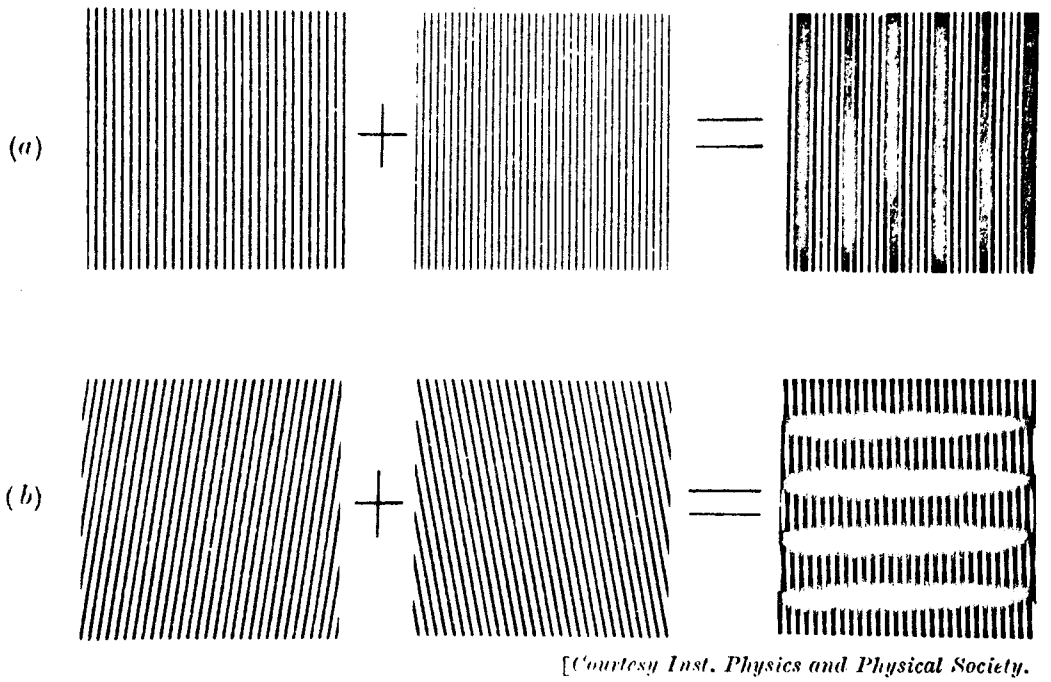

[*Courtesy Inst. Physics and Physical Society.*

Fig. 18. An optical analogue illustrating the formation of parallel and rotation moiré patterns. (*After Pashley.*)

(ii) deposition from the vapour phase on to a suitable substrate.

The instrumental resolution of modern electron microscopes is ~5 Å, but the resolution in the image is much poorer than this because of elastic and anelastic scattering of electrons in the specimen. It is therefore not possible to observe directly the atomic arrangement around

dislocations except in crystals with large lattice spacing. Such observations have been made on thin crystals of platinum phthalocyanine for which the atomic spacing is ~12 Å. Nevertheless, dislocations can be observed in metals where the spacing is only ~2 Å by magnifying the atomic displacements around the defect by means of a moiré-pattern technique. The principle of the method is illustrated in Fig. 18 for the analogue of two overlapping gratings. The moiré pattern represents the "beat" pattern that results from the two patterns going in and out of register in a periodic fashion. If two lattices with slightly different spacings d_1 and d_2 are allowed to overlap, the "parallel" moiré pattern then has a spacing D as shown in Fig. 18 by $D = d_1 d_2 / d_1 - d_2$. Alternatively a rotation moiré pattern can be produced by overlapping two lattices of the same spacing but rotated relative to each other by an angle α. In this case, the moiré pattern has a spacing D given by $D = d/\alpha$.

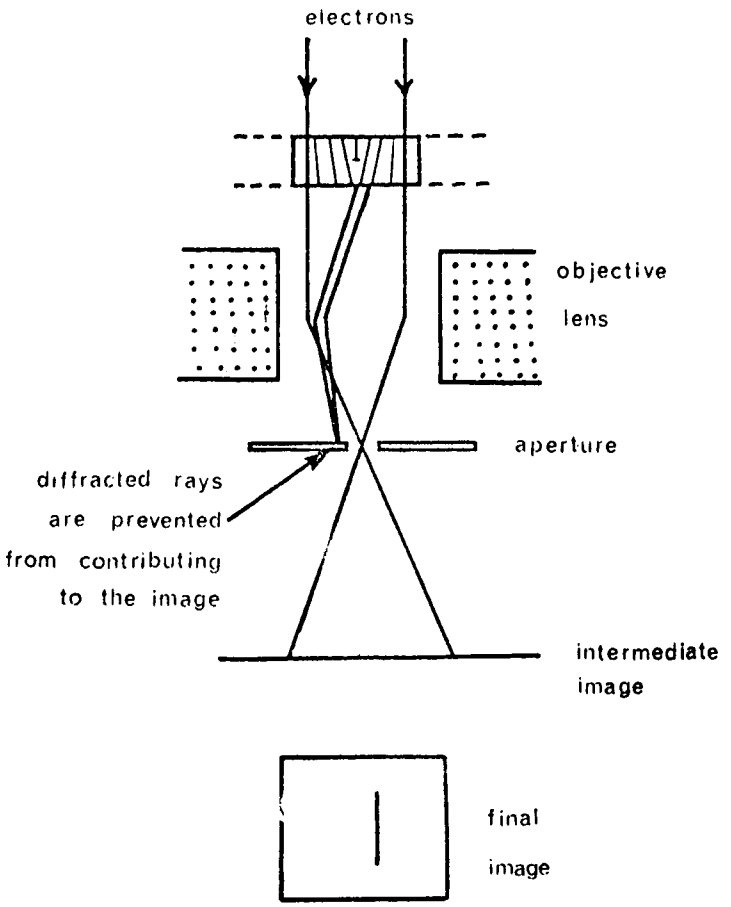

Fig. 19. Mechanism of diffraction contrast.

There are many examples of the moire technique applied to the study of precipitate/matrix interfaces, grain and sub-grain boundaries, and oriented deposits on substrates. These applications are limited, however, by the stringent requirements of the method. In general, therefore, the electron microscope is not used to resolve the lattice planes directly but instead dislocations and other defects are made visible in the instrument by means of Bragg diffraction of the electrons in the strain field around the dislocation core. This mechanism of diffraction contrast may be understood by reference to Fig.19 which shows the ray diagram for electrons passing through the objective lens of the microscope. All rays leaving the specimen in a particular direction are brought to a point of focus in the back focal plane of the objective lens; this gives an electron-diffraction pattern of the specimen from which it is possible to determine the orientation of the crystal and the (hkl) planes diffracting the electrons. The diffraction pattern and the image are magnified by two following projector lenses in the microscope. For normal bright-field microscopy an aperture is inserted in the back-focal plane centred over the main transmitted beam to allow the incident beam to pass through to the projector lenses but to block the diffracted rays. It follows that contrast arises in the bright-field electron optical image when regions of the specimen diffract (or reflect) electrons strongly, since a large part of the incident beam is then diffracted away and blocked by the objective aperture Fig. 19 . The planes diffracting electrons are those that obey the Bragg law and for 100-kV electrons ($\lambda \sim 0.04$ Å), $\theta \sim 1^{\circ}$ and hence in a perfect crystal the planes are those that are almost parallel to the electron beam. For a crystal containing a dislocation it is possible, using a goniometer specimen stage, to arrange for the general crystal orientation to deviate from the exact Bragg setting for reflection and hence to transmit a strong electron beam, while in the neighbourhood of the dislocation, but to one side, the reflecting planes are tilted into the reflecting position. Such a region therefore diffracts strongly relative to the surrounding perfect crystal and gives rise to a region of low intensity in the image. This region, usually ~ 100 Å in width, is the dislocation image.

The tilting of the reflecting planes near the dislocation core necessary to give a dislocation image can be seen in Fig.20. It also follows that

the dislocation image does not coincide with the actual dislocation line. The precise nature of the image depends on the diffracting conditions and varies with the different reflecting planes that can operate; under certain conditions it is visible. This condition arises when the reflecting planes are not tilted into the Bragg setting by the presence of the dislocation. Fig. 20 shows that this state of affairs prevails when the crystal planes reflecting the electrons contain the Burgers vector b; if g is a vector normal to the reflecting planes (hkl), then the invisibility condition is given by $g.b = 0$. The vector $g = 1/d_{hkl}$ is the reciprocal lattice vector normally used in diffraction theory.

Stacking faults also give rise to diffraction contrast effect. This is because the stacking-fault displacement vector R, defined as the shear parallel to the fault in that part of the crystal below the fault relative to that above the fault, which is regarded as fixed, gives rise to a phase difference $\alpha = 2\pi g.R$ in the electron waves diffracted from either side of the fault. The resultant diffracted beam from the fault depends on the depth of the fault in the specimen, so that the contrast observed is either uniformly bright or dark if the fault is parallel to the specimen surface, or takes the form of interference fringes running parallel to the intersection of the foil surface with the plane containing the fault. Such fringes are generally known as displacement fringes, and can occur whenever there is a displacement of the lattice across an inclined plane, such as takes place at twins, precipitates and grain boundaries.

An important application of thin-film transmission electron microscopy is in studying the distribution of dislocations in crystals after various thermal and mechanical treatments and the interactions between dislocations. In particular, contrast theory is used in the determination of the Burgers vector of any dislocations. It has already been mentioned that the contrast due to a dislocation becomes zero, i.e. the dislocation is invisible,*

* *This criterion is based on the known displacements around dislocations derived from isotropic elasticity, and is also valid for slightly anisotropic crystals. However, some intermetallic compounds are strongly anisotropic e.g. β-brass, and the invisibility criterion breaks down for such materials (see A.K. Head, M.H. Loretto, and P. Humble, Physica Status Solidi, 1967, 20, 505 521).*

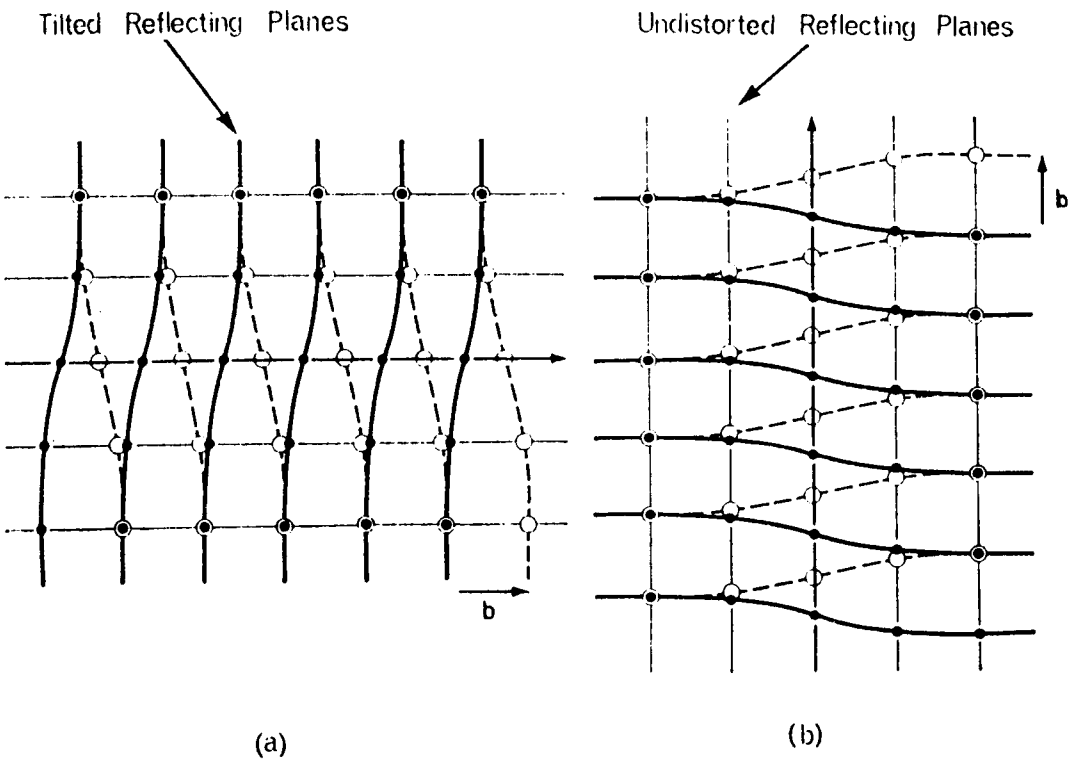

Fig. 20. Tilting of reflecting planes around a screw dislocation, oriented to produce: (*a*) contrast; (*b*) invisibility conditions.

when g.b. = 0. It follows therefore, that if the orientation of the specimen is changed until the dislocation goes out of contrast with a single strong reflection g operating, which may be determined from the selected-area diffraction pattern, then b lies in the reflecting plane for which g is the reciprocal lattice vector. In general, this information is sufficient to enable b to be determined, since b will be the shortest

lattice vector in the (hkl) plane identified by g. However, if another value of g can also be found to give invisibility, by further tilting of the specimen, then b lies along the line of intersection of the two reflecting planes identified. For example if $(h_1 k_1 l_1)$ and $(h_2 k_2 l_2)$ are the two reflecting planes that give invisibility then b = c $[uvw]$ is given by

$$[uvw] = [k_1 l_2 - l_1 k_2, l_1 h_2 - h_1 l_2, h_1 k_2 - k_1 h_2]$$

for a crystal structure of any symmetry.

The displacement vector R of a stacking fault can be determined in a similar way since g. R = 0 is the criterion for stacking-fault invisibility. In practice it is much easier to fulfil the condition giving zero contrast from the stacking fault even when $g.R \neq 0$. This condition will arise when the displacement vector R moves the imaging reflecting planes normal to themselves by a distance equal to a multiple of the spacing between the planes nd, and since $g = 1/d$ this condition is given by $g.R = n$, where $n =$ 1, 2, 3, &c.

9. DISLOCATIONS AND STACKING FAULTS IN TYPICAL METALLIC STRUCTURES

In a previous section we have considered some of the fundamental dislocation properties primarily based on a simple cubic structure. Real materials crystallize with more complex structures and in these the dislocations are also somewhat more complex. In this section the common metallic structure will be considered.

Face–Centred Cubic Structure

Unit Dislocation.

It is observed experimentally that in metals with f.c.c. structure slip takes place on a (111) plane in a ⟨110⟩ direction. The shortest

lattice vector in this structure is one joining a cube corner atom to a neighbouring face-centred atom and defines the observed slip direction; a dislocation with this Burgers vector $a/2$ $\langle 110 \rangle$ is called a perfect or unit dislocation. Fig. 21 shows the structure of an edge dislocation in the f.c.c. lattice, from which it is apparent that, in contrast to the simple cubic structure, the extra half-plane is now corrugated Fig 21. The corrugated plane of atoms is made up from a pair of $\{110\}$ -type atomic planes that occur in an ababab sequence, and consequently glide of the unit dislocation necessitates the movement of a pair of extra half-planes.

Shockley Partial Dislocations.

In practice, it is possible for the two $\{110\}$ planes of the pair of extra half-planes to glide separately. It then follows that the slip displacement produced by one of the extra half-planes will not correspond to a whole lattice vector, but instead to a partial lattice vector; hence the dislocation producing it is called a partial or Shockley partial dislocation. It also follows that the lattice in the wake of the moving partial dislocation will not have the correct f.c.c. stacking, but will contain a stacking fault. This stacking fault is shown in Fig. 21 as the ribbon between the two partial dislocations with Burgers vectors b_2 and b_3 respectively. By rearranging the structure in the core of the dislocation in this way, the severity of the distortion can be minimized by spreading the lattice disturbance over a plane rather than concentrating it along a line through the crystal. The energy gain may be estimated using Fig. 21 if it is considered that a unit dislocation with Burgers vector b_1 dissociates into partial dislocations with vectors b_2 and b_3 according to the reaction.

$$b \longrightarrow b_2 + b_3$$

A specific example of this reaction for dislocations in the (111) plane is

$$a/2\ [10\bar{1}] \longrightarrow a/6\ [2\bar{1}\bar{1}] + a/6\ [11\bar{2}] \qquad 10.$$

The correct indices for the vectors involved in such reactions can be deduced from a stereogram of the structure. However, it is worth noting that the dislocation reaction is (i) algebraically correct, since the sum of the components of the Burgers vector on both sides of the reaction are equal, as shown by

$$a/2\ [1,0,\bar{1}] \rightarrow a/6\ [2+1],\ a/6[\bar{1}+1],\quad a/6[\bar{1}+\bar{2}]$$

and (ii) energetically favourable, since the initial dislocation energy is proportional to $b_1^2 (= a^2/2)$ and the energy of the resultant partials to $b_2^2 + b_3^2 = a^2/3$. The pair of partials is coupled together by the stacking fault and the complete extended dislocation, as the configuration is called, glides as a single entity in the plane of dissociation, i.e. the slip plane.

The total energy E_T of the extended dislocation depends on the width of the stacking-fault ribbon w, according to

$$E_T = E_1 + E_2 + E_{12} + \gamma w$$

where E_1, E_2 are the energies of the individual partials, E_{12} is the interaction energy between them and γw is the energy of a unit length of fault with width w. The width of the fault may be estimated from a knowledge of the stacking-fault energy of the metal. When the distance separating the partials is w, the force of elastic repulsion, per unit length, between them is of the order of

$$\frac{\mu(b_2 \cdot b_3)}{2\pi w} = \frac{\mu a^2}{24\pi w}$$

and if the stacking-fault energy is γ, the force per unit length tending to bring the partials together is also γ. The equilibrium spacing is then given by

$$w = \frac{\mu a^2}{24\pi\gamma} \qquad \text{II.}$$

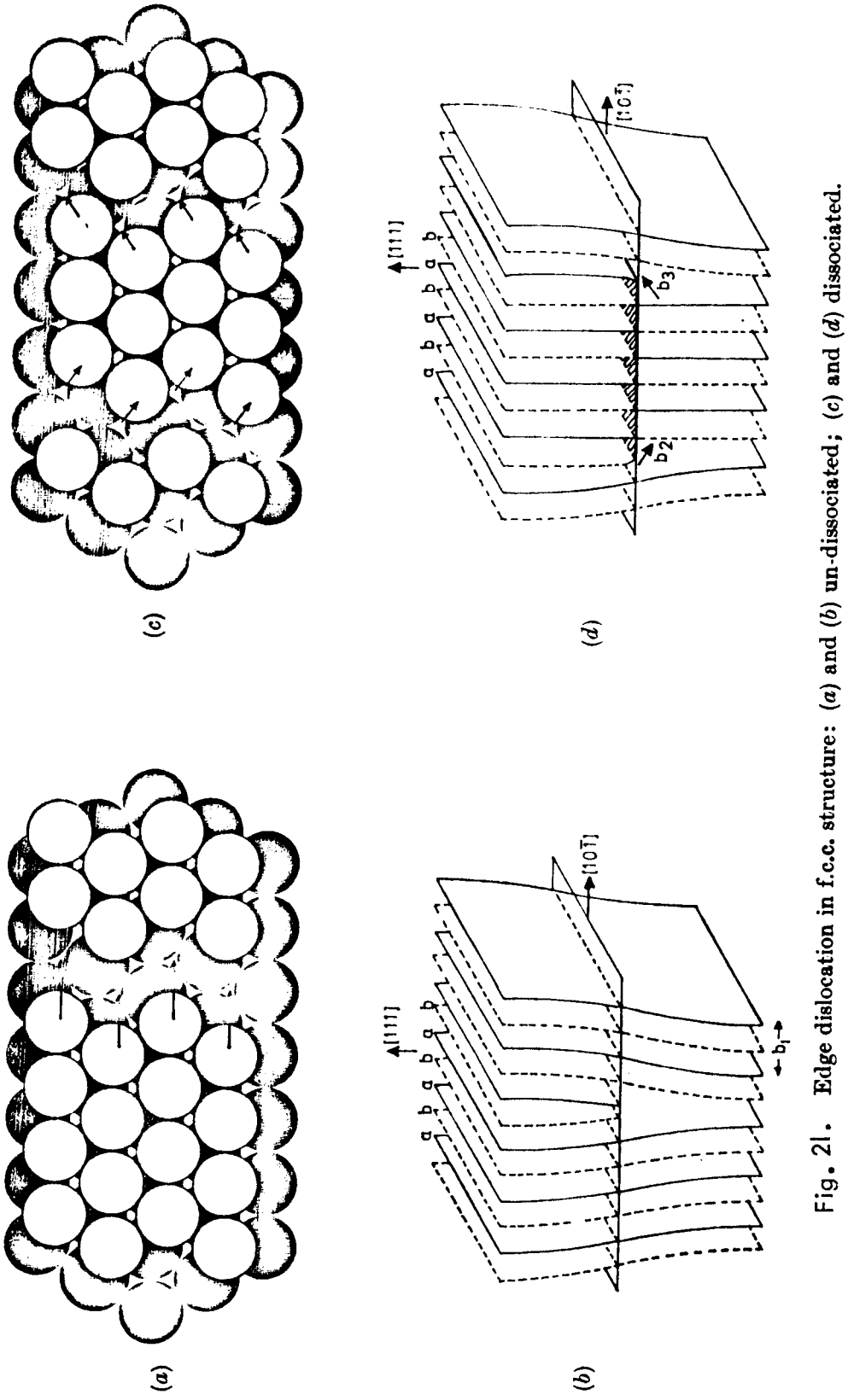

Fig. 21. Edge dislocation in f.c.c. structure: (*a*) and (*b*) un-dissociated; (*c*) and (*d*) dissociated.

For copper and aluminium, w is thought to be ~ 5 and 1 atomic spacings respectively.

Motion of Partials.

In general the dissociation of a dislocation confines the movement of the partials to glide in the plane containing the stacking fault; if the partials moved out of the plane of the fault, they would leave behind a high-energy surface of misfit, with energy probably as large as the grain-boundary energy γ g.b. (or 550 ergs/cm^2 for copper). The only way extended dislocations can change their slip plane is by first constricting to re-form a unit $a/2\langle 110\rangle$ dislocation, followed by dissociation of an intersecting plane. This cross-slip of an extended dislocation can occur only if the overall dislocation is screw in character and a possible sequence of events is illustrated in Fig. 22. It is imagined that the dislocation has been constricted along a

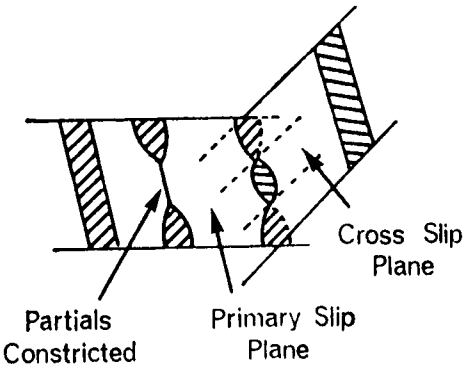

Fig. 22. Cross-slip of a dissociated screw dislocation.

short length because the extended dislocation is held up at some barrier in the lattice, and then the applied stress forces the partials together. The re-formed unit dislocation dissociates in the cross-slip plane and then glides as a new extended dislocation in the $(\bar{1}11)$ plane. The constriction necessary for the cross-slip process will be aided by thermal activation, and hence the

tendency to cross-slip decreases with decreasing temperature. The constriction is also more difficult to form, the wider is the separation of the partials; hence cross-slip is less frequent in metals of low stacking-fault energy.

Frank Partial Dislocations.

In the above example, the Burgers vector of the partial lies in the fault plane and hence it is capable of gliding. However, when the vector does not lie in the fault plane it cannot glide, and hence it is sessile. Such a dislocation, introduced by Frank, can be produced by removing part of a close-packed layer of atoms from the crystal by aggregating excess vacancies, produced for example by quenching from a high temperature, to form a disc-shaped void that subsequently collapses to give an edge dislocation loop Fig. 16. Alternatively, a Frank partial dislocation can be formed by inserting part of an extra layer of atoms obtained by aggregating interstitials (produced, for example, by irradiation with high-energy particles) between two normal planes of atoms. In each case, the Burgers vector of the dislocation is $a/3\ [111]$, i.e. normal to the (111) plane of the fault and equal in magnitude to the spacing of the close-packed planes. Although such dislocations cannot glide, then can climb by the addition or removal of vacancies or interstitials respectively.

The Frank dislocation loop of either type contains a stacking fault. For the vacancy loop, by removing a layer of atoms, e.g. a B-layer, the stacking sequence changes from the normal ABCABCABC to ABCACABC. For the interstitial loop, by inserting a B-layer the sequence becomes ABCBABC. These faults are called intrinsic and extrinsic stacking faults, respectively. Similarly, an A- or C- layer could be removed instead of a B-layer to give other intrinsic faults, and an A-layer inserted between B- and C-layers or a C-layer between A- and B-layers to give other extrinsic faults. When describing stacking faults it is convenient to use the notation, due to Frank,* where the symbol Δ denotes any translation between atomic planes in the sequence A $\longrightarrow$ B $\longrightarrow$ C $\longrightarrow$ A that gives the normal stacking sequence $\Delta\,\Delta\,\Delta\,\Delta$ for an f.c.c. crystal, and ∇ denotes any translation C $\longrightarrow$ B $\longrightarrow$ A $\longrightarrow$ C that would give $\Delta\Delta\Delta\nabla\Delta\Delta\Delta$ for the intrinsic fault sequence and $\Delta\Delta\nabla\nabla\Delta\Delta$ for the extrinsic fault sequence.

It is evident that a stacking fault can be formed either by means of a partial shear $a/6\ \langle 112 \rangle$ on a $\{111\}$ plane or by the aggregation of point

*

F.C. Frank, "Symposium on Plastic Deformation of Crystalline Solids", p. 89. 1950: Washington D.C. (Office of Technical Services, U.S. Dept. of Commerce).

defects on such a plane. A single $a/6$ ⟨112⟩ shear produces an intrinsic fault indicated by ABCA↓CABC or ΔΔΔ▽ΔΔΔ, which is geometrically equivalent to that produced by the collapse of a single platelet of vacancies. If a second shear is performed on the plane above the first the stacking sequences becomes ABCA↓C↓BCA or ΔΔΔ▽▽ΔΔ and an extrinsic stacking fault is formed, which is equivalent to that produced by either aggregating a single platelet of interstitials on a close-packed plane or a second platelet of vacancies on the intrinsic fault produced by the first platelet of vacancies. The schematic structure of such a double dislocation loop is shown in Fig. 17 and examples of single-faulted (Frank) loops and double-faulted loops have been observed in quenched aluminium. The observation of double-faulted loops indicates that it is energetically more favourable to nucleate a Frank sessile dislocation loop on an existing intrinsic fault than randomly in the perfect lattice, and it therefore follows that the energy of the double, or extrinsic, fault is somewhat lower than twice that of the intrinsic fault, i.e. γ ext. $< 2\gamma$ int. This has been confirmed by loop-annealing experiments, as discussed on page 47.

If the shear $a/6$ ⟨112⟩ is carried out plane by plane above A the stacking sequence becomes ABCA↓C↓B↓A↓C↓B and a coherent twin is produced. The twin is thus equivalent to a series of intrinsic stacking faults on neighbouring planes. In principle, such a twin could be produced by the aggregation of vacancy platelets on neighbouring planes; Fig. 17 shows that two intrinsic faults on neighbouring planes produce an extrinsic fault, and the addition of a third intrinsic fault would produce a coherent twin, which would be energetically favourable since γ twin $< \gamma$int. $< \gamma$ext.. It is possible, however, to reduce the energy of the crystal further by aggregating the third layer of vacancies between the two previously formed neighbouring intrinsic faults according to the following sequence

ABCABCABCABC	perfect crystal
ABCA↓CABCABC	single (intrinsic) fault
ABCA↓C↓BCABC	double (extrinsic) fault
ABCA↓↓↓BCABC	perfect crystal

rather than the twin fault

ABCACBABC coherent twin

The aggregation of vacancies to produce perfect crystal by means of a three-layer sequence has been observed in slowly quenched aluminium* and in aluminium-magnesium alloys+.

Lomer-Cottrell Sessile Dislocation.

Sessile, i.e. immobile, dislocations may also be formed by the interaction of two glissile (mobile) dislocations. A typical example is the interaction between dislocations on intersecting $\{111\}$ planes, such as those gliding in the $(11\bar{1})$ and (111) planes. The two unit dislocations are dissociated according to (Fig. 23).

$$a/2\ [01\bar{1}] \rightarrow a/6\ [\bar{1}2\bar{1}] + a/6\ [11\bar{2}]$$

in (111) and

$$a/2\ [10\bar{1}] \rightarrow a/6\ [2\bar{1}\bar{1}] + a/6\ [112]$$

in $(11\bar{1})$, and under suitable conditions it is possible for the partials to combine according to

$$a/6[\bar{1}2\bar{1}] + a/6[2\bar{1}1] \rightarrow a/6\ [110]$$

leaving the other two partials unaffected by the reaction. The new partial with vector $a/6\ [110]$ is called a stair-rod dislocation, since it lies along the line of intersection of two stacking faults. It is a very low-energy dislocation with $|b| = a\sqrt{2}/6$ and since its Burgers vector does not lie in either of the $\{111\}$ planes but in the (100) plane it is sessile. Together with the coupled partials the stair-rod dislocation forms what is commonly called a Lomer-Cottrell barrier. Such barriers have been observed by electron metallography in stainless steels that have low stacking-fault

* *J.W. Edington and D.R. West, Phil. Mag. 1966, 14, 603.*
\+ *S. Kritzinger, R.E. Smallman and P.S. Dobson, Acta Met. 1968, 16, in the press.*

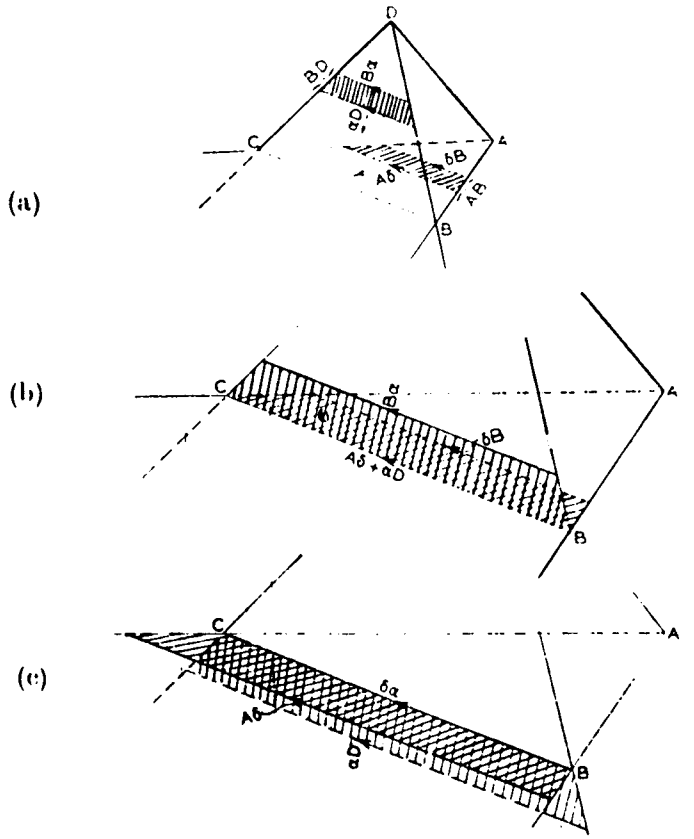

[*Courtesy North-Holland Publishing Co.*

Fig. 23 Lomer–Cottrell barrier formed by the interaction of an extended dislocation on the (111) plane, *DBC*, with one on the (11$\bar{1}$) plane *ABC*. The dislocations and stacking faults are given by lines and shading; the lettering refers to the Burgers vectors in terms of the Thompson relation (see below). (*After Kuhlmann-Wilsdorf.*)

energies, and are important in some theories of work-hardening in f.c.c. crystals.

Thompson Reference Tetrahedron.

All the dislocation structures observed in f.c.c. crystals can be conveniently discussed in terms of a simple geometrical representation first proposed by Thompson,* and since called the Thompson tetrahedron. This tetrahedron is constructed from the four different {111} planes such that the edges of the tetrahedron lie along ⟨110⟩ directions in these planes, as shown in Fig. 24. The faces are labelled at their mid-points

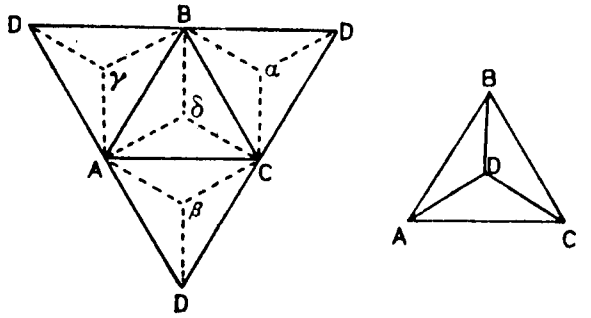

Fig. 24. The Thompson tetrahedron *ABCD*. The tetrahedron is also shown on the left opened out.

by α β γ and δ, and the vertices opposite these faces by A, B, C, and D (D being below the plane ABC). The faces of the tetrahedra may be considered as (111) glide planes and the edges glide directions, equal in length to a $a/\sqrt{2}$, which is the magnitude of the Burgers vector of a unit dislocation $b = a/2$ ⟨110⟩. The Burgers vectors of the various dislocations can then be represented in the following manner:

*N. Thompson, Proc. Phys. Soc., 1953, [B], 66, 481.

(1) Unit dislocations of the type $a/2\langle 110\rangle$ by the edges AB, BC, &c., the letters and the order in which they are written covering the twelve cases.

(2) Shockley partial dislocations into which the unit dislocations are dissociated, by $B\alpha$, αC, $B\gamma$, γC, &c. In any one slip plane - α, for example - we have $B\alpha + C\alpha = \alpha D$, the sum of two displacements is equal to the negative of the third. The dissociation reaction given by equation 10 can then be represented by

$$BC \longrightarrow B\alpha + \alpha C$$

where BC represents the unit dislocations in the α plane and $B\alpha$ and αC the two Shockley partials produced by the dissociation. It can easily be seen that in any given (111) plane there are six possible dissociation reactions. The lettering of the partial dislocations can be carried out correctly (for intrinsic faults) applying Thompson's rule, which states that for an observer situated outside the reference tetrahedron, looking down on the slip plane in the positive direction of the dislocation, the right-hand partial bears the Roman-Greek symbol and the left-hand partial the Greek-Roman symbol.

The cross-slip reaction discussed previously can be represented in this notation by a dissociated screw dislocation, say, $B\alpha + \alpha C$ in the α plane, cross-slipping into the δ plane by first constricting into the unit dislocation BC and then dissociating in the δ plane into the partials $B\delta$ and δC according to

$$B\alpha + \alpha C \longrightarrow BC \longrightarrow B\delta + \delta C$$

(3) The Frank partial dislocation has its Burgers vector perpendicular to the (111) plane on which it lies and is represented by αA, βB, γC, or δD. Loops of edge dislocation formed on (111) planes by the condensation of vacancies are commonly observed in quenched f.c.c. metals, as shown in Fig. 17. Often the stacking fault can be removed by a shearing stress across the plane of the fault, giving rise to the spontaneous nucleation and growth of a Shockley partial in the fault plane. In this case, the Shockley partial combines with the Frank partial to give a unit dislocation according to a reaction of the type

$$A\alpha + \alpha B \longrightarrow AB$$

The unit dislocation lies on the α plane with Burgers vector AB and hence is a prismatic dislocation loop; the higher strain energy of the prismatic is compensated by the elimination of the stacking fault. The reaction is therefore particularly favourable in metals with high stacking-fault energy.

(4) Stair-rod dislocations which exist at the intersection of stacking faults on intersecting $\{111\}$ planes can also be represented by the Thompson tetrahedron. The simplest is formed at an acute-angled intersection, for example between dislocations on the δ plane and the α plane Fig. 23. Dislocations on the δ plane and α plane can dissociate according to

$$AB \longrightarrow A\delta + \delta B \qquad \text{(on the } \delta \text{ plane)}$$

$$BD \longrightarrow B\alpha + \alpha D \qquad \text{(on the } \alpha \text{ plane)}$$

and when the two Shockley partials δB and $B\alpha$ interact, a stair-rod dislocation with Burgers vector $\delta\alpha = a/6\ \langle 110\rangle$ will be produced. This dislocation has very low energy and is pure edge because $\delta\alpha$ is perpendicular to its line BC; it is therefore sessile. If the other pair of partials interact then the resultant Burgers vector of the stair-rod will be $(A\delta + \alpha D)$ which is of higher energy and of the form $a/3\ \langle 110\rangle$. This vector may also be written in Thompson's notation as $A\alpha/\delta D$ and is a vector equal to twice the length joining the mid-points of $A\alpha$ and δD.

Table 2. Dislocation Vectors in the F.C.C. Lattice

Type	Burgers Vector	Symbol	Relative Energy
Unit dislocation	$a/2\ \langle 110\rangle$	AB	1
Shockley partial	$a/6\ \langle 112\rangle$	$A\delta$	1/3
Frank partial	$a/3\ \langle 111\rangle$	δD	2/3
Stair-rod at acute bend	$a/6\ \langle 110\rangle$	$\alpha\delta = \alpha B + B\delta$	1/9
Stair-rod at obtuse bend	$a/3\ \langle 100\rangle$	$BC/\delta C = B\delta + C$	2/9
Stair-rod at acute bend	$a/3\ \langle 011\rangle$	$A\alpha/\delta D = A\delta + \alpha D$	4/9
Stair-rod at obtuse bend	$a/6\ \langle 301\rangle$	$AB/\delta\alpha = A\delta + B\alpha$	5/9

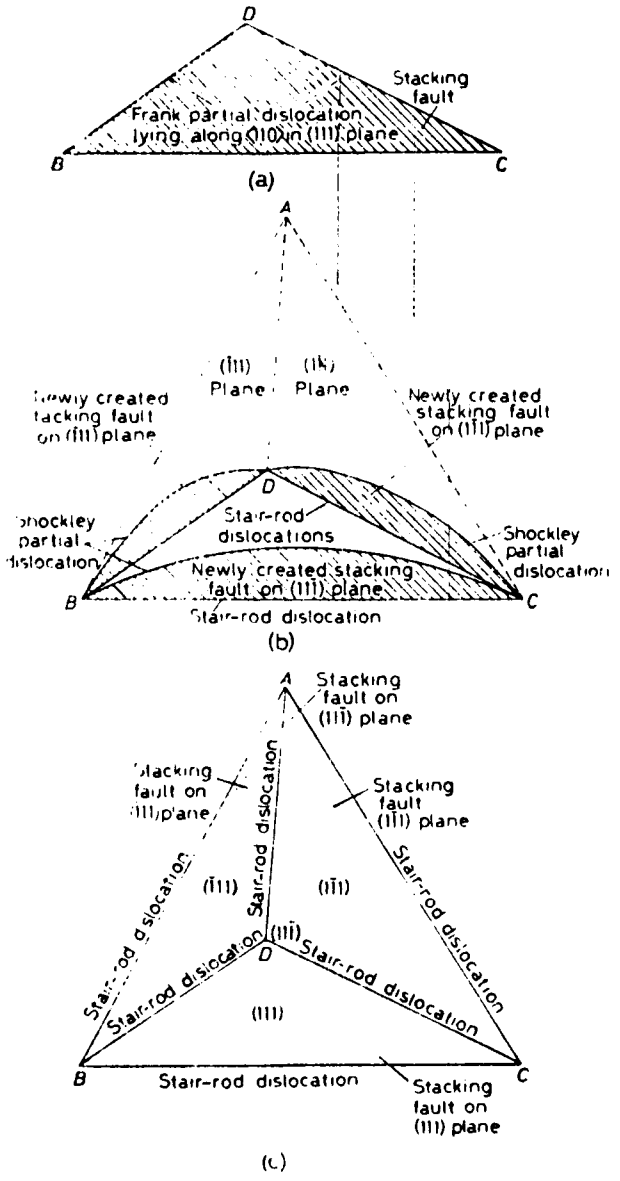

[*Courtesy Butterworths.*

Fig. 25. Formation of defect-tetrahedron. (*a*) Frank sessile dislocation loop; (*b*) dissociation of Frank partials; (c) defect tetrahedron. (*After Smallman.*)

For the intersection at an obtuse angle of A_δ and B_α the Burgers vector of the stair-rod is $(A\delta + B\alpha)$ or $AB/\delta\alpha$ and has a vector of the form $a/6\ \langle 301\rangle$. The partial $B\delta$ may also interact with C_α to give $BC/^{\delta\alpha}$ with a Burgers vector of the form $a/3\ \langle 100\rangle$. The various types of dislocation that could exist in the f.c.c. lattice are tabulated, Table 2 together with their Burgers vectors and relative energies.

Defect Tetrahedron.

In metals with low stacking-fault energy, such as gold or silver, three-dimensional defects may be formed in the shape of a tetrahedron of stacking faults on $\{111\}$ planes with $a/6\ \langle 110\rangle$ stair-rod dislocations along the edges of the tetrahedron Fig. 23

There are at least two ways in which such tetrahedra may be formed. Perhaps the easiest to understand is from the dissociation of a Frank partial dislocation, as originally proposed by Silcox and Hirsch.* Suppose, for example, a Frank loop forms on a (111) plane by the aggregation of vacancies and to lower its energy is triangular in shape with edges parallel to the three $\langle 110\rangle$ directions, AB, BC, and CA, in the (111) plane. A frank dislocation with Burgers vector $a/3\ \langle 111\rangle$, or δD if it forms on the δ plane of the Thompson tetrahedron, can lower its energy by dissociating into a Shockley partial and a stair-rod according to

$$\delta D \longrightarrow \delta\gamma + \gamma D \qquad \text{(for the dislocation along AB)}$$
$$\delta D \longrightarrow \delta\alpha + \alpha D \qquad \text{(for the dislocation along BC)}$$
$$\delta D \longrightarrow \delta\beta + \beta D \qquad \text{(for the dislocation along CA)}$$

where the dislocations with Burgers vectors $\delta\gamma$, $\delta\alpha$, and $\delta\beta$ are stair-rod dislocations and those with vectors γD, αD, and βD are Shockley partials glissile in the γ, α, and β planes respectively. Geometrically, as shown in Fig. 25 this means that each of the three Shockley portials glides away from the original plane of the loop leaving behind a stair-rod at the position formerly occupied by the Frank loop, and creating new stacking fault on the three intersecting α, β, and γ planes. At the line of intersection of the α-β, β-γ, and γ-α planes the Shockley partials combine

*J. Silcox and P.B. Hirsch, Phil. Mag. 1959, 4, 72.

to produce three additional stair-rod dislocations, $\gamma\alpha$, $\alpha\beta$, and $\beta\gamma$. The defect then consists of a tetrahedron of stacking faults with stair-rod dislocations along its six edges.

More recently, deJong and Koehler* have proposed that in quenched specimens the tetrahedron forms by growth rather than by dissociation, and that the nucleus for a tetrahedron is a small, three-dimensional vacancy cluster. The smallest cluster that is able to collapse to a four-atom tetrahedron and subsequently grow by the absorption of vacancies is a hexa-vacancy. Then, since only single, di-, and tri-vacancies are present in a specimen immediately after quenching, the nucleation of a tetrahedron requires the formation of a tetra-vacancy by di-vacancy coalescence or a single vacancy with a tri-vacancy, which by combination with a di-vacancy gives a hexa-vacancy. Support for the growth mechanism is now quite strong, since tetrahedra approaching 3000 Å in size have been observed in gold, which is much larger than the 400-500 Å expected from the dissociation mechanism, and few tetrahedra are observed+ in quenched specimens that have been up-quenched to 100°C where the tetra-vacancy complex is unstable. Recent observations‡ have also shown that the tetrahedra grow in the presence of an excess vacancy concentration.

Although tetrahedra probably form by growth following a quenching treatment, the tetrahedra produced by deformation no doubt form by a dissociation mechanism.

Measurement of Stacking-Fault Energy.

Compared to incoherent interfaces and boundaries (i.e. free surfaces and grain boundaries) the energies of coherent boundaries, (i.e., twins and stacking faults) are quite low, because there the atomic structure is very much less disordered. The surface energy of a metal is given approximately by the relation $\gamma_s \sim \mu b/8$ and the grain-boundary energy has been estimated in Section 6 to be γ g.b. $\sim \mu b/20$, or about one-third that of the surface energy.

*M. de Jong and J.S. Koehler, Phys. Rev., 1963, 129, 40, 49.
+R. Segall and L. Clarebrough, Phil. Mag., 1964, 9, 865.
‡I. Johnston, P.S. Dobson and R.E. Smallman, unpublished work.

For copper, the experimental values are $\gamma_s \sim 1750$ ergs/cm^2 and γ g.b. ~ 550 ergs/cm^2. The stacking-fault energy is therefore expected to be $\gamma_{s.f.} \sim 100$ ergs/cm^2 and, in fact, values for different metals and alloys range from a few ergs/cm^2 to a few hundred ergs/cm^2.

The energy of a stacking fault can be estimated from twin-boundary energies since a stacking fault ABCACABC may be regarded as two overlapping twin boundaries CAC and ACA, across which the next-nearest neighbouring planes are wrongly stacked. In f.c.c. crystals any sequence of three atomic planes not in the ABC or CBA order is a stacking violation and is accompanied by a distortional energy contribution. A twin has one pair of second nearest neighbour planes in the wrong sequence, two third neighbours, one fourth neighbour, and so on; an intrinsic stacking fault has two second nearest neighbours, three third, no fourth nearest neighbour violations, and an extrinsic fault has two second nearest neighbour, four third, and three fourth violations. Thus, if next-next nearest neighbour interactions are considered to make a relatively small contribution to the energy, then an approximate relation $\gamma_I = \gamma_E = 2\gamma_T$ is expected to be obeyed. The results given in Table 3 show that this is a reasonable approximation in most metals, although for some metals such as nickel the agreement is poor.

Table 3 Twin Energies, Stacking-Fault Energies and Dislocation Widths of Some Common F.C.C. Metals

Metal	γ_T, ergs/cm^2	$\gamma_{s.f.}$ ergs/cm^2	w/b
Ag	15	20	9.0
Au	33	45	3.1
Cu	22 - 32	80	3.5
Ni	26 - 51	240	2.1
Al	71	135	1.08

The free energies of interfaces can be determined from the equilibrium form of the triple junction where three interfaces, such as surfaces, grain boundaries, or twins, meet. For the case of a grain boundary intersecting a free surface, shown in Fig. 26 then

$$\gamma_{g.b.} = 2\gamma_s \cos \theta/2,$$

and hence γ g.b. can be obtained by measuring the dihedral angle θ and knowing γ_s. Similarly, measurements can be made of the ratio of twin-boundary energy to the average grain-boundary energy, and in cases where an absolute value of the latter is known, an estimate of γ_T and thus $\gamma_{s.f.}$ can be made Table 3. In general, the abundance of annealing twins observed in f.c.c. metals and alloys is a good quantitative guide to the fault energy, and shows for example that $\gamma_{Al} > \gamma_{Cu} > \gamma_{\alpha\text{-brass}}$.

High-resolution electron transmission microscopy has now made it possible to observe directly stacking faults and widely dissociated dislocations in various crystals and an estimate of $\gamma_{s.f.}$ can be made from such observations. It is not possible, however, to obtain reliable values merely by measuring the width of an extended ribbon, since the width is sensitive to local stress conditions in the thin foil. Instead, it is necessary to make measurements on equilibrium stacking-fault configurations such as those observed in dislocation networks lying in (111) planes in f.c.c. crystals. When an extended dislocation on the α-plane with Burgers vector $DC \longrightarrow D\alpha + \alpha C$ Fig. 22 intersects a dislocation on the δ-plane with

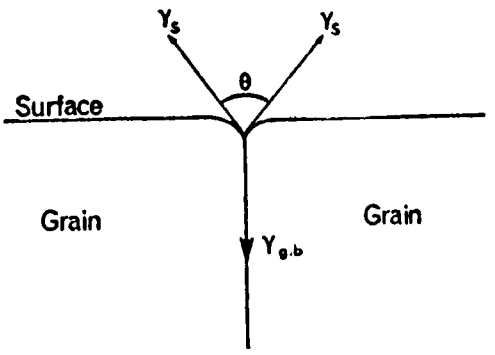

Fig. 26.

vector $CB \longrightarrow C\delta + \delta B$, the dislocations constrict at the intersection and then CB dissociates in the α plane to $C\alpha + \alpha B$ combining spontaneously with the αC of the intersected dislocation to produce the dislocation αB. This partial αB is then pulled down in the α plane and the resultant dislocation network takes the form shown in Fig. 27 of extended and contracted nodes; when the common partials of two extended dislocations lie on the same side of the node an extended node is formed, but when they lie on opposite sides, the node is contracted. From a measurement of either the radius of curvature R or the width W of an extended node it is possible to obtain a measure of the stacking-fault energy of the metal or alloy. This follows because the force per unit length tending to straighten the dislocation line at the node ($F = T/R$, where T is the line tension and R the radius of curvature) is balanced by the opposing force per unit length γ due to the stacking fault tending to contract the node. In equilibrium the radius of curvature of the node is given by

$$R = T/\gamma \sim \mu b^2/k\gamma$$

where k depends on the character of the dislocation at the node.

The node method suffers from being limited to materials having $\gamma/\mu b < 3 \times 10^{-3}$, the upper limit for which extended nodes are observed in the microscope. For values of γ/μ b up to $\sim 10^{-2}$ a method based on the observation of fault tetrahedra has been proposed which in its present form involves the measurement of the maximum size of stacking-fault tetrahedron and the minimum size of Frank loop formed by deformation. It is assumed that Frank loops are formed from a glissile dislocation containing a sessile jog and if the Frank loop is less than a critical size it will dissociate by the reaction discussed on page 41 to form a stacking-fault tetrahedron. The energy path involved in this dissociation has been analysed and the calculations allow a value of $\gamma/\mu b$ to be determined from the maximum edge length of the tetrahedron (L_T).

For intermediate and high stacking-fault energy values a method

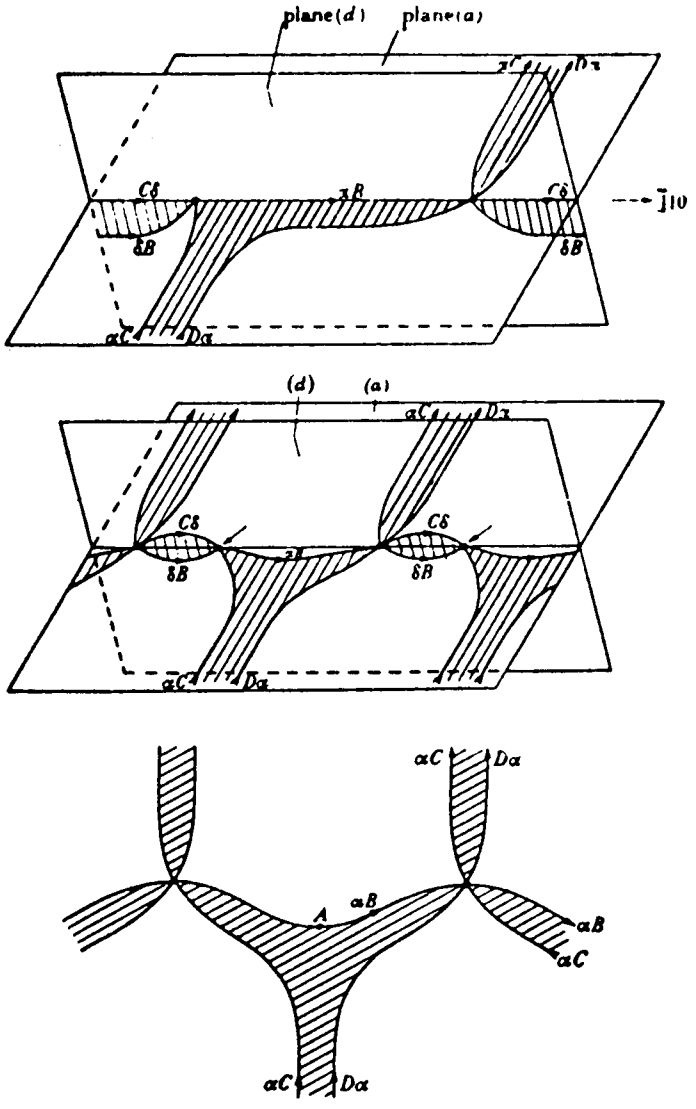

[*Courtesy Royal Society.*

Fig. 27. Formation of extended nodes. (*After Whelan.*)

based on the annealing of faulted dislocation loops has been developed by Smallman and his co-workers. On heating a metal foil containing such loops, vacancies are emitted and the loops shrink by climb. The driving

force for the climb process F_c arises from the line tension of the dislocation and the stacking fault and is given by

$$F_c = \left\{\mu b^2/4\pi r\ (1 - \nu)\right\} \ln \left[r/b\right] + \gamma \qquad 12.$$

At large loop sizes the contribution from the fault far outweighs that due to the dislocation, so that $F_c \sim \gamma$, and in principle the stacking-fault energy can be determined from measurements of the climb rate of faulted dislocation loops. In thin foils it is observed that the diffusion of vacancies to the foil surface controls the climb of dislocation loops and for large faulted loops the annealing rate is given by

$$(dr/dt)_F = -2\pi D/b \ln\left[t/b\right]\left\{\exp\ (\gamma B^2/kT) - 1\right\} \qquad 13.$$

where $D = a^2 \nu \exp\ (-E_D/kT)$ is the coefficient of self-diffusion, and t the foil thickness. The pre exponential factors in the rate equation can be obtained by control experiments on unfaulted dislocation loops and a value of $\gamma\ I_{s.f.} = 135 \pm 20$ ergs/cm^2 has been deduced for the intrinsic stacking-fault energy. Similar annealing experiments on extrinsically faulted loops in aluminium give $\gamma^E{}_{s.f.} = 180 \pm 20$ ergs/cm^2.

Dislocations in Hexagonal Structures

In a hexagonal close-packed structure the most closely packed plane of atoms is the basal plane (0001) and the most closely packed directions $\langle 11\bar{2}0\rangle$, which of course lie in the basal plane. The smallest unit lattice vector is $a/3\ \langle 11\bar{2}0\rangle$ and hence the usual slip dislocation has a Burgers vector $a/3\ \langle 11\bar{2}0\rangle$ and glides in the (0001) plane. Other dislocations do exist, however, and these can be represented in a notation similar to that for the f.c.c. structure, but using a double tetrahedron instead of the single tetrahedron discussed for f.c.c. structures. The double tetrahedron*, is shown in Fig. 23 and its use leads to the following simple types of dislocation: 28

(i) Six perfect dislocations with Burgers vectors in the basal plane along the sides of the triangular base ABC. They are AB, BC, CA, BA, CB and AC.

*A. Berghezan, A. Fourdeux and S. Amelinckx, Acta Met. 1961, 9. 464.

(ii) Six partial dislocations with Burgers vectors in the basal plane represented by the vectors $A\sigma$, $B\sigma$, $C\sigma$, and their negatives. These dislocations arise from dissociation reactions of the type

$$AB \longrightarrow A\sigma + \sigma B$$

(iii) Two perfect dislocations perpendicular to the basal plane represented by the vectors ST and TS of magnitude equal to the cell height c.

(iv) Partial dislocations perpendicular to the basal plane represented by the vectors σS, σT, $S\sigma$, $T\sigma$ of magnitude $c/2$.

(v) Partial dislocations represented by vectors AS, BS, CS, AT, BT, and CT. Although these vectors represent a displacement from one atomic site to another, the resultant dislocations are imperfect because the two sites are not identical. Such dislocations could eventually dissociate according to

$$AS \longrightarrow A\sigma + \sigma S,$$

but since the resultant Burgers vector are mutually perpendicular, the stability of AS cannot be decided on the basis of energy proportional to the square of the Burgers vector. The energies of the various dislocations are given on a relative scale in

Table 4. Dislocations in the Hexagonal C.P. Structure

Type	AB	$A\sigma$	ST	σT	AS
Direction .	$[11\bar{2}0]$	$[\bar{1}100]$	$[000\bar{1}]$	$[000\bar{1}]$	$[\bar{2}203]$
Strength .	a	$a/3$	c	$c/2$	$\sqrt{(a^2/3 + c^2/4)}$
Energy .	a^2	$a^2/3$	$c^2 = 8a^2/3$	$2a^2/3$	a^2

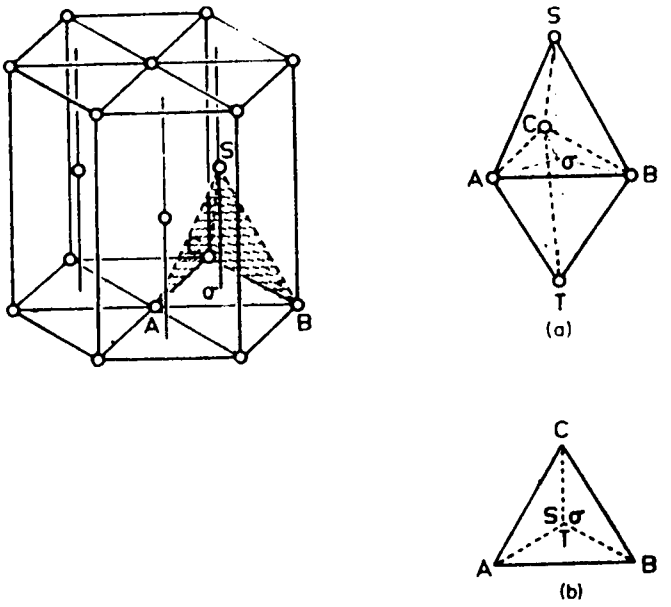

[*Courtesy "Acta Metallurgica"*.

Fig. 28. Double tetrahedron for hexagonal lattices. (*After Berghezan, Fourdeux, and Amelinckx.*)

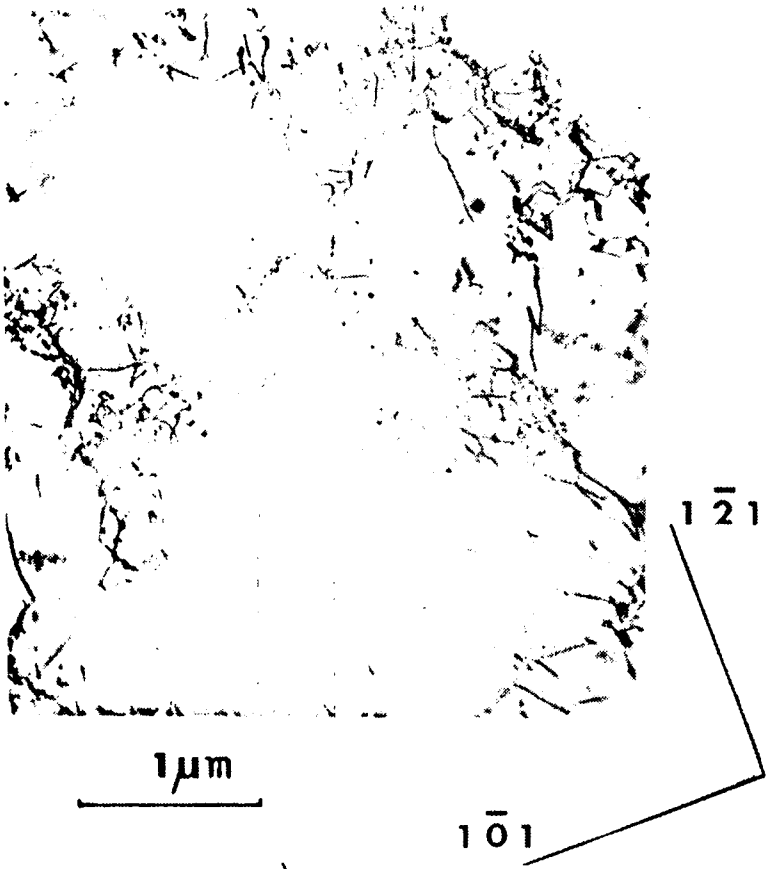

c)

d)

If instead of the ideal axial ratio $c/a = 1.633$ the real value is used, then the values of ST, T σ, and AS will be increased by a small amount for c/a greater than ideal and reduced for c/a less than ideal.

There are many similarities between the dislocations in the h.c.p. and f.c.c. structure and, as a consequence, it is not necessary to discuss them in great detail. However, it is instructive to consider the two basic processes of glide and climb.

Dislocation Glide.

A perfect slip dislocation in the basal plane AB = $a/3\ [11\bar{2}0]$ and this can dissociate into two partials separating a ribbon of stacking fault by a reaction

$$AB \longrightarrow A\sigma + \sigma B$$

This is identical with the reaction in the f.c.c. lattice and the width of the stacking-fault robbon is again inversely proportional to the stacking-fault energy. There are very few measurements of γ for hexagonal metals but careful observations* by means of the loop-annealing techniques show that γ for zinc is 140 ergs/cm^2 and for magnesium 125 ergs/cm^2. Dislocations in these metals are therefore not normally widely dissociated. A screw dislocation lying along a $[\bar{1}2\bar{1}0]$ direction is capable of gliding in the three different glide planes but the extension in the basal plane will be sufficient to make basal glide easier than either pyramidal $(10\bar{1}1)$ or prismatic $(10\bar{1}0)$ glide. Pyramidal and prismatic glide will be more favoured at high temperatures in metals with very high stacking-fault energy. It is also observed that non-basal slip is favoured in metals with $c/a < 1.633$.

Dislocation Climb.

In hexagonal lattices, if vacancies aggregate as a platelet, as shown in Fig. 29 the resultant collapse of the disc-shaped cavity would bring two similar layers into contact, which is a situation incompatible with close-packing and indicates that simple Frank dislocations are possibly energetically unfavourable in h.c.p. lattices. This unfavourable situation can be removed by either of two

* *P.S. Dobson and R.E. Smallman, Proc. Roy. Soc. 1966, [A] 293, 423.*
J. Harris and B. Masters, ibid., 1966 [A] 292, 240.
R. Hales, R.E. Smallman, and P.S. Dobson, ibid., 1968, [A], in the press.

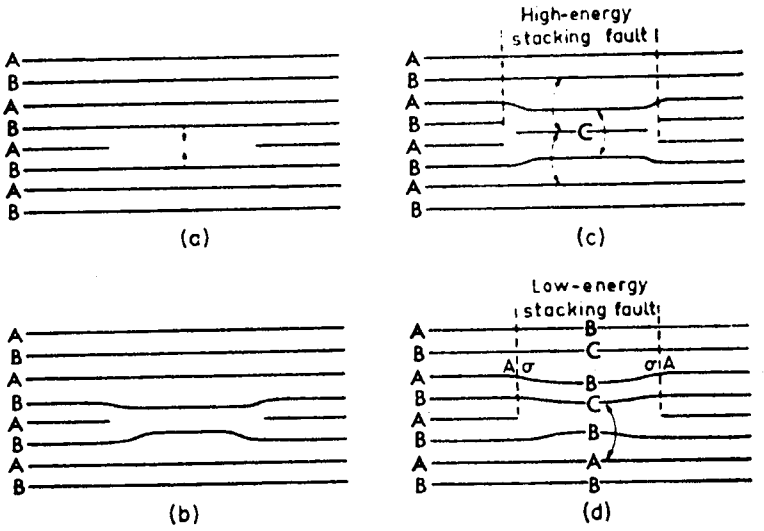

Fig. 29. Dislocation-loop formation in hexagonal lattices.

mechanisms, in Fig. 29(c) the stacking of a B layer is changed to a C position. The Burgers vector of the dislocation loop will be of the σS type and the energy of the fault will probably be high because of the three next-nearest neighbour violations. In Fig. 29 (d) the loop is swept by a partial dislocation which changes the stacking of all the layers above the loop according to the rule $A \rightarrow B \rightarrow C \rightarrow A$. The Burgers vector of the loop is of the type AS, from the dislocation reaction $A\sigma + \sigma S \longrightarrow AS$, and the associated stacking fault should have an energy somewhat less than the previous example because there is only one next-nearest neighbour violation in the stacking sequence. In zinc these faulted dislocation loops are capable of growth or shrinkage by climbing during the addition or removal of point defects to the dislocation line, as studied in some detail for zinc by Dobson and Smallman.

10. THE STRENGTHENING OF METALS

Ideal Crystals.

The ease with which metal crystals can be plastically deformed at stresses many orders of magnitude less than the theoretical strength ($\tau_m = \mu\, b/2\pi a$) is quite remarkable. This property is due to the gliding

ability of a dislocation in a periodic crystal structure as illustrated in Fig. 30. At symmetrical positions in the lattice, indicated in Fig. 24 the dislocation is in neutral equilibrium, because the atomic forces acting on it from each side are balanced. As the dislocation moves from these symmetrical lattice positions some imbalance of atomic forces does exist, but this is quite small, particularly in wide dislocations where the transition from the slipped to the unslipped region is spread over several (e.g. five or more) atom distances in the crystal Fig. 31. The wider the dislocation the more nearly do the atomic forces acting on the dislocation from either side cancel. The perfect crystal lattice therefore offers very little resistance to the motion of a dislocation, and hence it is capable of moving, like an elastic wave, at very high speeds through the crystal.

Direct measurement of dislocation velocity v have now been made in some crystals by means of the etch-pitting technique; the results of such experiment are shown in Fig. 32 . Edge dislocations move faster than screws and the velocity of both varies rapidly with applied stress τ according to

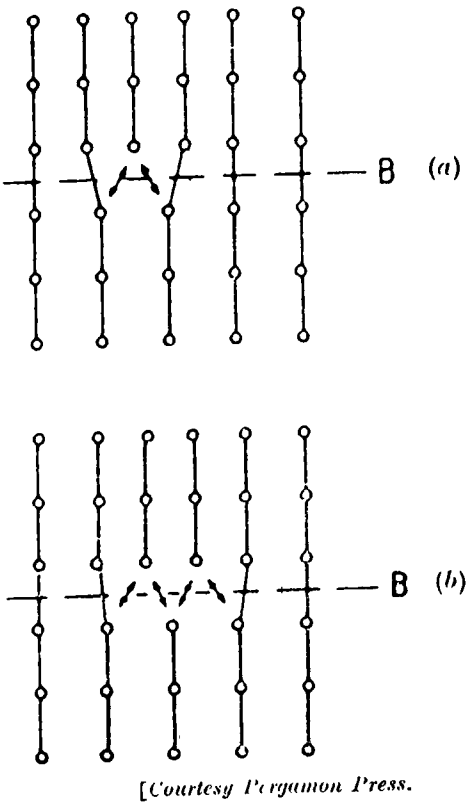

[*Courtesy Pergamon Press.*

Fig. 30. Equilibrium positions for a dislocation. (*After Gilman.*)

an empirical relation of the form

$$v = (\tau/\tau_0)^n \qquad 14.$$

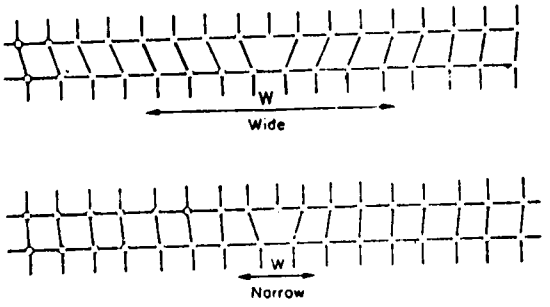

[*Courtesy Inst. Mech. Eng.*

Fig. 31. Wide and narrow edge dislocations. (*After Cottrell.*)

where τ_0 is the stress for unit speed and n is an index that varies for different materials. The index n is usually low ($\sim$ 2) for intrinsically hard, co-valent crystals such as germanium, between 10 and 40 for b.c.c. crystals, and high ($\sim$200) for intrinsically soft f.c.c. crystal. A critical stress is required to start the dislocations moving and denotes the onset of plastic deformation. The yield stress detected in a macroscopic tensile test is a relatively insensitive measure of the onset of plastic deformation and is related to the dislocation moving at some finite velocity (e.g. $\sim$ 100 Å/sec). Calculations of the influence of temperature on velocity for several different materials indicate that the lower the test temperature the higher is the stress

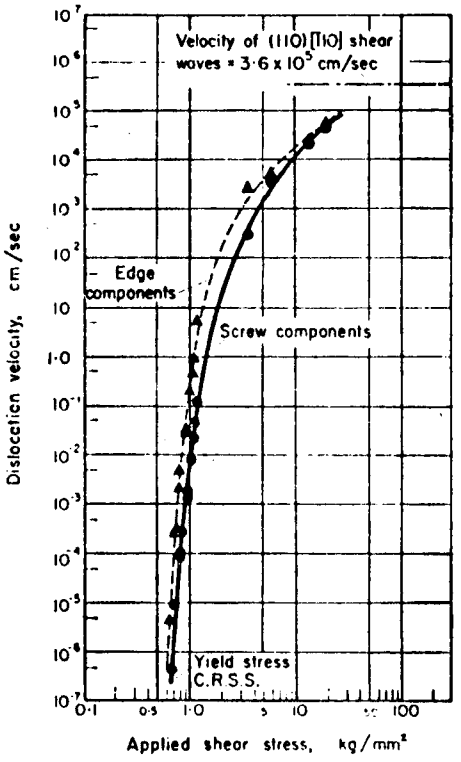

[*Courtesy "J. Appl. Physics".*

Fig. 32 Dislocation speeds in LiF.
(*After Johnston and Gilman.*)

level required to produce the same finite velocity, which is consistent with the increase in yield stress with decreasing temperature. In general, the dislocation mobility is related to the temperature-dependence of the stress for gliding and is small for f.c.c. crystals but large in most other crystals, particularly at low temperatures.

In contrast to the theoretical strength, τ_m, the intrinsic strength of a crystal is the stress to move an existing dislocation in an otherwise perfect crystal. This stress depends sensitively on the width w of a dislocation, since we have seen that w governs the dislocation mobility, and the simple sinusoidal force-distance relationship used in section I to calculate τ_m is

given by Peierls and Nabarro* as being of the form

$$\tau_{p.n.} \simeq \mu \exp\left[-2\pi w/b\right] \qquad 15.$$

with

$$w = \mu b/2\pi(1-\nu) \quad \tau_m = a(1-\nu)$$

where a is the interplanar spacing and ν is Poisson's ratio, indicates that the two opposing factors affecting w are (i) the elastic energy of the crystal, which is reduced by spreading the elastic strains out, and (ii) the misfit energy, which depends on the number of misaligned atoms across the slip plane. Metals with close-packed structures have dislocations that are extended in close-packed planes; moreover, since these planes are the most widely spaced, i.e. have a small b/a factor, the alignment forces are weakest between them. These metals have highly mobile dislocations and are intrinsically soft. In contrast, directional bonding in crystals tends to produce narrow dislocations, which leads to intrinsic hardness and brittleness. Extreme examples are the co-valent crystals such as diamond and silicon and ceramic crystals. Eshelby+ has shown that the mobility of a dislocation is given by

$$S = 4\pi (w/b) \exp\left[-2\pi w/b\right] \qquad 16$$

where w (= K $d/2c$) is the width of the dislocation, and c is the shear modulus in the glide direction on glide planes of spacing d.

Because of their intrinsic softness, most metals and alloys in commercial application are hardened by placing obstacles in the paths of glide dislocations to hinder their motion. The most common obstacles are lattice defects such as

*R.E. Peierls, Proc. Phys. Soc., 1940, 52, 34.
F.R.N. Nabarro, ibid, 1947, 59, 256.
+J. Eshelby, Phil. Mag. 1949, 40, 903.

other dislocations (although a dislocation weakens a perfect crystal the addition of more dislocation brings about a strengthening, because the dislocations mutually obstruct one another), grain boundaries, and impurities or solute atoms.

Real Crystals.

The movement of individual dislocations has been discussed in sections 2 and 4. The amount of slip produced by a single-unit dislocation is small and in practice the plastic deformation of crystals must involve the movement of very many dislocations; for example, a slip step, visible under the light microscope as a slip line, must be at least 3000 Å in height and hence ~ 1000 dislocations must have glided in a given slip band. In general, the total shear strain produced will be the sum of the contributions from all the individual dislocations that have moved. Suppose in Fig.33 that, instead of a single-unit dislocation there are

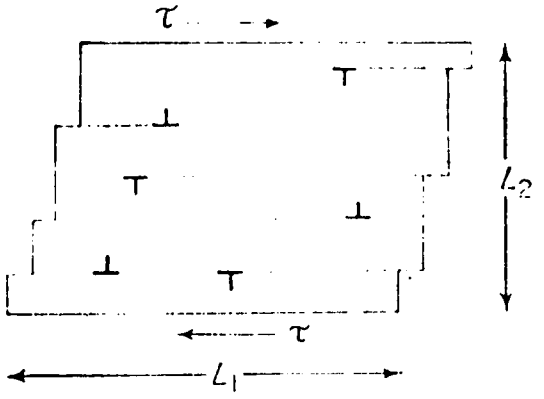

Fig. 33. Shear produced by gliding dislocations.

$\rho L_1 L_2$ dislocations moving, where ρ is the density* of dislocations defined as the number of dislocations threading unit area of the specimen. If these

*ρ is also defined as the total length of dislocations in unit volume, i.e. ρcm of dislocation line per cm^3, i.e. ρ/cm^2.

move completely across the crystal the shear strain will be

$$\gamma = \rho L_1 L_2 (b/L_2)$$

but if the average distance each dislocation moves is $\bar{x}$ then the average shear strain will be

$$\gamma = \rho L_1 L_2 (b/L_2)(\bar{x}/L_1) = \rho b \bar{x} \qquad 17.$$

If the dislocations move 10^{-4} cm. which is the size of an average sub-grain then the maximum strain produced by 10^8 dislocations per cm^2, the density usually observed in annealed crystals, is only a fraction of 1% ($\gamma = 10^8 \times 3 \times 10^{-8} \times 10^{-4}$) even if they are all capable of gliding. In practice, plastic strains of > 100% can be achieved and to produce these large strains the in-grown dislocation must multiply during straining. Some of the mechanisms whereby dislocations originate have been outlined in Section 7. However, to explain the movement of large numbers of dislocations in a given slip band the concept of a dislocation source has been introduced.

The principle of the dislocation source, first discussed by Frank and Read,* is illustrated in Fig. 34. The dislocation line PQ of length l lies in a slip plane represented by the plane of the paper and is held at both ends by some sessile lattice feature such as a dislocation node or multiple jog. Under the action of an applied shear stress the dislocation bows out, as shown in Fig. 34 the radius of curvature decreasing with increasing stress τ according to the relation $R = \mu b/\tau$. The dislocation adopts a semicircular form Fig. 34 when $\tau = \mu b/l$ and with further increase in stress the dislocation line expands as shown in (c) and (d). Between positions (c) and (d) parts of the loop that approach each other below the line PQ meet and annihilate each other to form a closed loop. By this process the original dislocation source is regenerated inside a continuous loop. The process can therefore be repeated and a series of loops generated, each loop producing unit slip as it expands in the slip plane.

Direct observations have shown that in metals with high stacking-fault energy, e.g. b.c.c. metals and in ionic and co-valent materials, a modification of the Frank-Read source mechanism operates. In this case the source dislocation

*F.C. Frank and W.T. Read, Phys. Rev. 1950, 79, 722.

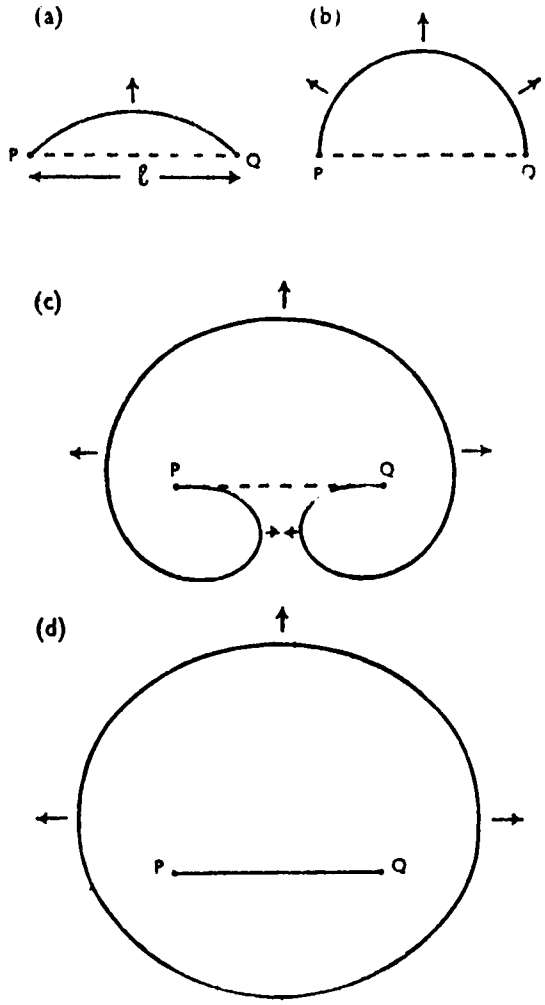

Fig. 34. Frank–Read source.

is formed by the repeated cross-slip of lengths of screw dislocations, as shown in Fig. 35. The source, anchored by multiple jogs lying in the cross-slip plane, expands in the manner described above. The screw components of the expanding

glide loop are capable of cross-slipping again to form a new source and the whole process can be repeated by cross-glide multiplication. In this way a single dislocation loop is able to expand, multiply, and spread to neighbouring parallel slip planes to produce a wide slip band.

Dislocations are able to multiply by climb as well as glide, provided that a supersaturation of vacancies is present in the vicinity of the dislocation. The precipitation and clustering of vacancies in the lattice give rise to monolayer cavities that subsequently collapse to dislocation loops, as already discussed. When the vacancies precipitate on dislocations that are initially in, or near, pure screw orientation, helical dislocations are formed by climb as originally suggested by Seitz*. The helices may be considered, formally, as the

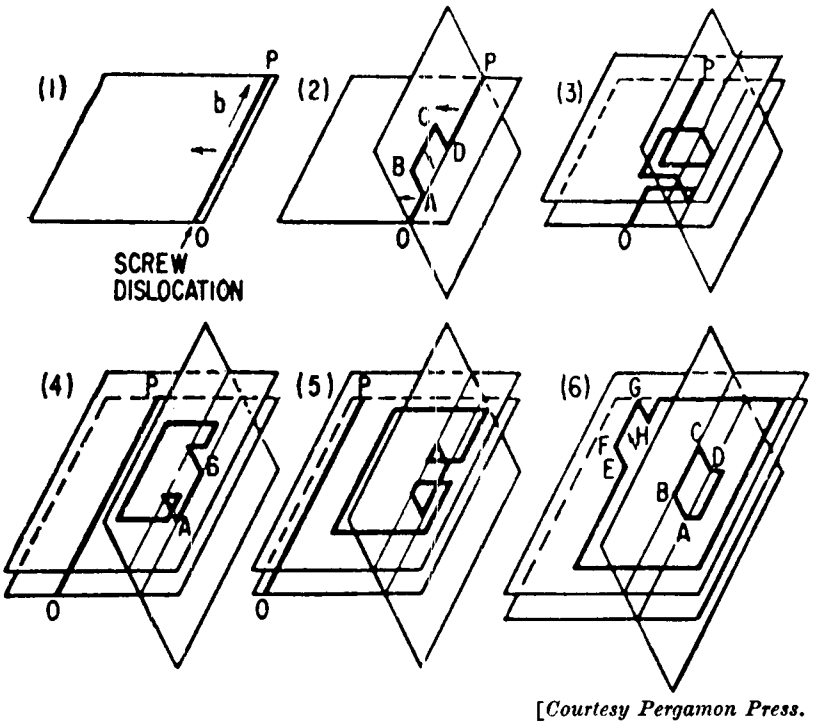

[*Courtesy Pergamon Press.*

Fig. 35. Cross-glide multiplication of dislocations. (*After Gilman.*)

result of the interaction of a row of prismatic loops with the original screw dislocation, as shown in Fig. 36. When the vacancies precipitate on to an edge dislocation a climb source may operate. The operation of such a

*F. Seitz, *Advances in Physics*, 1952, 1, 43.

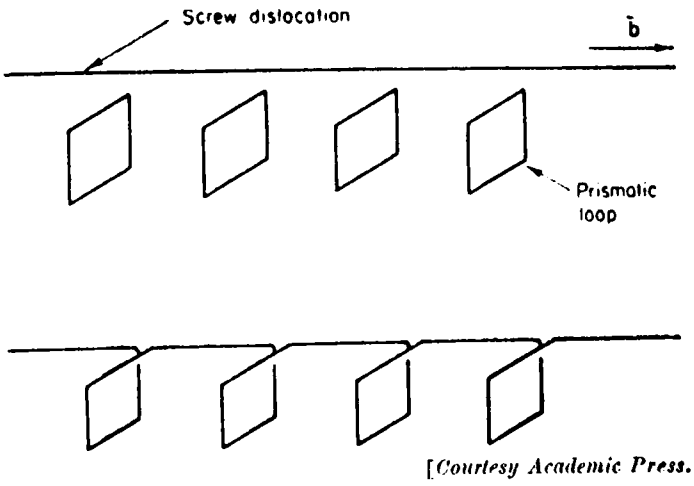

Fig. 36. (*After Smallman and Eikum.*)

Bardeen-Herring source is the climb equivalent of the slip source proposed by Frank and Read. The source dislocation pinned at its ends moves in a plane perpendicular to the Burgers vector, i.e. by climb, as a result of

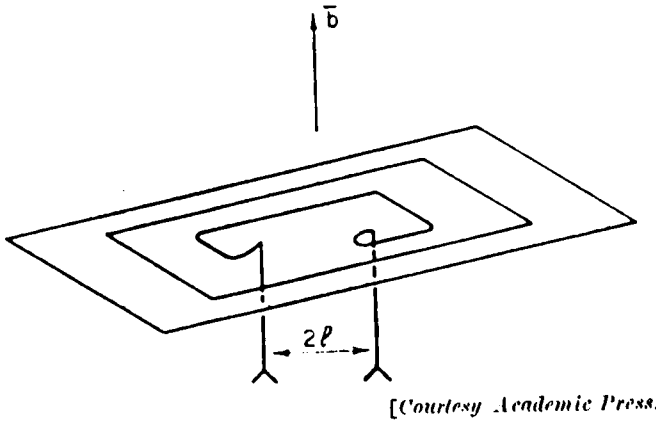

Fig. 37. (*After Smallman and Eikum.*)

vacancies condensing on to it, and not, as in the slip case, by the movement in the plane containing the Burgers vector. The process is shown schematically in Fig. 37. Bardeen and Herring did not discuss the nature of the anchoring points of the source dislocation, but the source must end on dislocations having a screw component if it is to remove more than one plane of atoms. This new type of source was originally detected and investigated by Westmacott, Barnes and Smallman* and has since been observed by several other workers.

Alloy Hardening.

The addition of solute atoms to a crystal increases the stress to move a dislocation and thereby causes hardening. The increase in glide stress arises from several causes, one of the main contributions being the interaction of the added atom with glide dislocations through their elastic strain field. The extent of the hardening depends, however, on the distribution of alloying atoms and for a random solid solution is weak because, on the average, the force exerted by an atom against the dislocation is countered by an equal and opposite force on the dislocation from an atom behind it. In contrast, a non-random distribution of solute gives rise to a greater hardening. Such a distribution is produced by ageing the alloy at a suitable temperature to allow the atoms to diffuse and segretate either (i) on dislocations or (ii) into small groups or clusters. Clustering commonly occurs following the ageing of a supersaturated solid solution and the hardness associated with the process is known as precipitation-hardening.

The segregation of solute atoms to dislocations takes place to relieve the distortion that surrounds a given solute atom in the perfect lattice. Thus, a substitutional solute atom bigger than the solvent atom will tend to segregate to sites in the expanded region below the extra half-plane of an edge dislocation and small substitutional atoms to the compressed region; interstitial atoms will tend to segregate into the large interstitial site below the half-plane.

The phenomenon of the sharp yield point in iron or mild steel has been attributed to the segregation of carbon and nitrogen atoms to dislocation in iron. Fig. 38 is a typical stress/strain curve showing that the stress drops sharply from the upper yield point A to the lower yield point B, to be followed

*K.H. Westmacott, R.S. Barnes and R.E. Smallman, Phil. Mag. 1962, 7, 1585.

by the yield elongation BC when a macroscopic band of deformation, known as a Luders band, propagates down the tensile specimen at approximately constant stress, before the specimen work-hardens, CD. Cottrell and Bilby[+] proposed that, after annealing, dislocations in iron are immobilized by atmospheres of carbon or nitrogen atoms and on straining are unable to move at the stress at which a free dislocation would normally glide. On raising the stress to the ultimate yield point the dislocations are torn away from their atmospheres and once free, the stress to continue dislocation glide is lower than that to start glide. If an overstrained specimen (curve 2) is immediately retested, no yield point is observed because the dislocations are free from impurity locking and simply continue their glide motion. However, if a specimen is aged (e.g. 10 min or more at 100°C for iron) to allow the impurity atoms to segregate again on the dislocations, the yield point reappears on straining (curve 3). This process is known as strain-ageing and the increase in strength associated with the return of the yield point is known as strain-age-hardening. It is now known that the

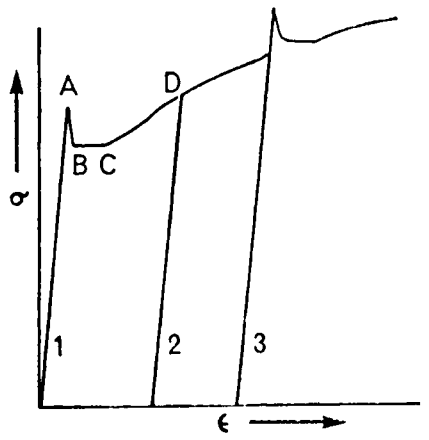

Fig. 38.

Cottrell-Bilby theory holds only for conditions of weak locking, i.e., very short ageing times. This point is discussed in more detail in the section on polycrystals on page 71.

[+] *A.H. Cottrell and B.A. Bilby, Proc. Phys. Soc., 1949, [A], 62, 49.*

The segregation of solute atoms in the lattice gives rise to precipitation or dispersion-hardening. Common examples in practice are to be found in many aluminium alloys, which are first quenched from ~ 500°C to retain the solute elements, particularly copper, in supersaturated solid solution and then aged at ~ 150-200°C to precipitate the solute atoms in a controlled manner. For light ageing treatments the copper atoms, for example, cluster into platelets coherent with the {100} planes of the aluminium matrix, but on subsequent ageing the clusters, or zones as they are called, grow into incoherent zones and finally definite precipitates.

Initially, the strength of the alloy is that of a supersaturated solid solution and the contributions to the strength are those that arise in general for solid solutions. The shear strain at a distance of r from a solute atom of radius r_0 is $\varepsilon r_0^3/r^3$ and this gives rise to an average internal stress $\tau_i = \mu\varepsilon c$, where c is the solute concentration and ε $(= 1/a\ da/dc)$ the misfit. Mott and Nabarro* identify this internal stress with the flow stress of the alloy when the minimum radius of curvature to which dislocations can be bent by the internal stress is smaller than the mean separation d of the stress centres, which in this case are solute atoms. The minimum radius of curvature, R, is related to the line tension of the dislocation and the stress value by

$$\tau_i b = TR \qquad 18.$$

which for $T \sim \frac{1}{2}\mu b^2$ gives $d \gtrsim b/4c$; typically $\varepsilon = 0.1$, $c = 0.02$, and hence $d_c \sim 100b$. In solid-solution alloys or alloys containing very finely dispersed precipitates, d is very small ($\sim b/c^{1/3}$) and therefore the local stress fields are not sufficiently large to bend a dislocation around each individual stress centre (Fig. 39). The line cannot follow the sharply changing stress field and hence has to override the stress field. Thus, under stress, a finite length L of dislocation line has to move to allow the centre to move through a distance d from one equilibrium position to the next. The line experiences a non-vanishing stress of magnitude

$$\tau_c = \tau_i d/4L \simeq \mu\varepsilon^{4/3} c \qquad 19.$$

N.F. Mott and F.R.N. Nabarro, "Report of a Conference on Strength of Solids", p.1 1948: London (Physical Society).

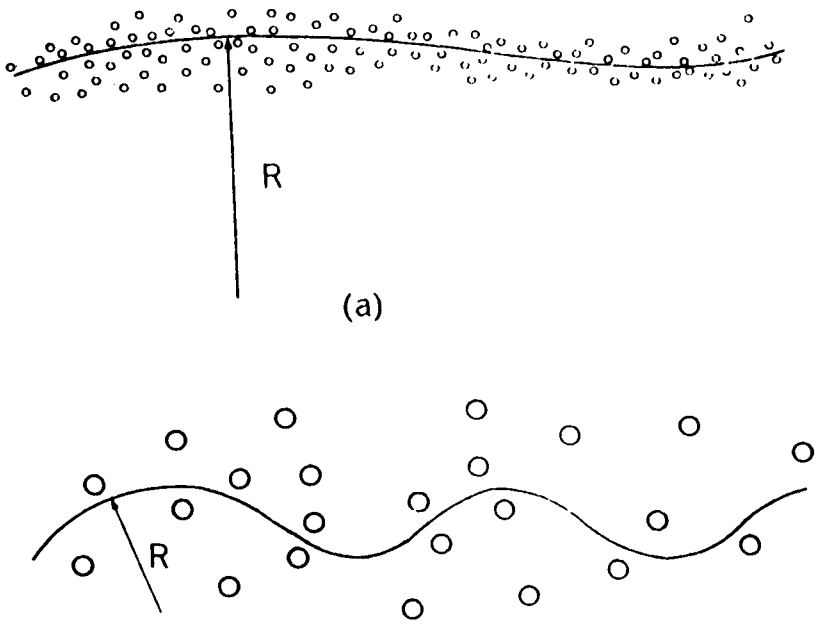

Fig. 39. Interaction of dislocation with precipitates.

A somewhat larger value of $\tau_c \simeq \mu\varepsilon c$ is obtained if L is taken to be the radius into which the average internal stress bends the dislocation. Such a theory predicts that solid-solution hardening is directly proportional to the solute concentration c and this is generally observed in practice. However, the theory overestimates the flow stress in f.c.c. alloys, but gives more nearly the correct magnitude in b.c.c. alloys.

Additional contributions to the flow stress can arise from solute atoms: (i) by virtue of an inhomogeneity interaction with the dislocation, and (ii) from the presence of short-range order. The former has been considered

by Fleischer[+] in terms of the difference in shear modulus between the solute atom and the matrix, to account for the hardening in copper- and silver-based alloys by a combination of size interaction with screw dislocations and shear modulus. However, recent work[*] shows that the Fleischer analysis of solution-hardening is not applicable to silver-base alloys. In the case of ordered alloys, long-range order is overcome by the motion of super-dislocations but when short-range order exists in an alloy the passage of a single dislocation will destroy the local order across the slip plane, producing a more nearly random higher-energy configuration. Thus, if γ_D is the disordering energy per unit area of slip plane, this will be the work done in moving a unit length of dislocation across unit distance of the slip plane τb, and hence

$$\tau = \gamma_D / b \qquad 20.$$

It is considered that short-range ordering is responsible for a significant part of the yield stress of α-brass.

Precipitation often first takes place by the formation of small clusters of solute atoms or zones that are coherent with the matrix, and hence are cut by dislocations moving in the matrix lattice. This behaviour is confirmed by electron-microscope observations. Clearly, if the dimensions of the zones or precipitates is small in the direction of cutting, the strength will be temperature-dependent. In general, therefore, the yield stress at this stage is governed by the stress necessary to force dislocations through the precipitate, contributions to which may arise from the elastic strain field near the precipitate, the disordering of the precipitate structure when the matrix dislocations pass through, and any difference in elastic modulus or stacking-fault energy[**] between the precipitate and the matrix.

[+] *R.L. Fleischer, Acta Met., 1961, 9, 996; 1963, 11, 203; J. Appl. Physics, 1962, 33, 3504.*

[*] *M.M. Hutchinson and R.W.K. Honeycombe, Metal Sci. J., 1967, 1, 70.*

[**] *P.B. Hirsch and A. Kelly, Phil. Mag., 1965, 12, 881.*

The elastic strain provides a significant contribution to the yeild stresses in alloys such as aluminium-copper containing zones, often termed G.P. zones after Guinier and Preston who first detected them, or precipitates, and copper-beryllium alloys, where the precipitates are coherent with the matrix lattice, and this is given by

$$\tau = 2\mu\varepsilon f \qquad 21.$$

where $\varepsilon = 1/a\ da/dc$ is the misfit of the particle in the matrix and f is the volume fraction of precipitate or dispersed phase. The maximum contribution arises when the particles reach a critical dispersion such that the dislocations are able to bend around individual particles, i.e. $R = d \sim 100b$, (Fig. 39). However, even for such dispersions the dislocations have to cut through the precipitates and are subject to considerable short-range interactions. These involve disruption of the atomic bonds at the surface and inside the precipitates such that the flow stress is given by

$$\tau = \alpha\gamma_D f^{\frac{1}{2}}/b \qquad 22.$$

Here γ_D is a measure of the disorder created by the dislocation and includes the energy of the additional matrix-precipitate formed by shear, the disorder energy due to change of nearest-neighbour atoms across the slip plane, and the energy of any interface dislocations formed. This type of chemical hardening is important in aluminium-based alloys with silver and zinc and in Nimonics* with Ni_3Al precipitates, where the particle/matrix misfit is small. An additional contribution to the flow stress may arise from the difference in stacking-fault energy $\gamma_{s.f.}$ between the matrix and the particle,+ particularly in alloys where the other strengthening mechanisms do not predominate. The effect arises from the different dislocation width inside the particle and in the matrix and predicts a variation in the flow stress with particle size according to

$$\tau = \alpha\Delta\gamma_{s.f.}\ r/bd \qquad 23.$$

Trade name of Henry Wiggin and Co. Ltd.,

+*P.B. Hirsch and A. Kelly, Loc. Cit.*

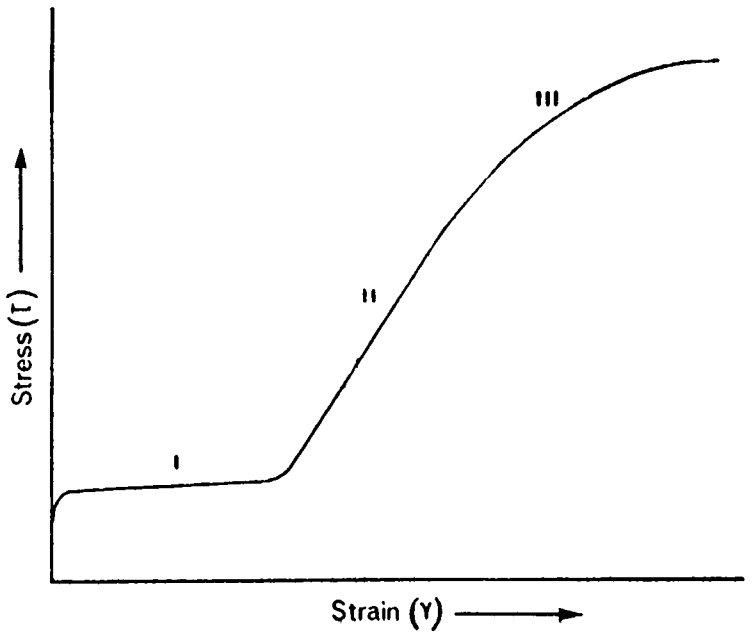

Fig. 41. Schematic stress/strain curve from f.c.c. crystal, showing 3-stage hardening.

where L is the separation between the particles. With such a dispersion the specimen is said to be overaged. As shown in Fig.40 when the dislocation by-passes the particle a dislocation loop is left around it, and with the passage of successive dislocations many such loops are formed. Thus, concurrently with the decrease in yield stress the rate of work-hardening increases if the particles are sufficiently strong, because of the turbulent flow around them. These loops also produce a stress in the particle which is much higher than on the slip plane as a whole. This effect, in which the particles act like rigid pegs across the slip plane, was first discussed by Fisher, Hart, and Pry and is known as the (F.H.P.) effect. The limiting strength of the alloy is controlled by this effect, since if the particles are weak they yield or break under the stress from the pile-up of loops. Very strong solids with strengths of the order of $10^{-2}\,\mu$ can be produced with 10% volume fraction of particles, in a very finely dispersed form.

Work-Hardening

In general, the multiplication of dislocations during plastic deformation increases the stress necessary for dislocation motion. This is known as work-hardening and the magnitude of the hardening depends sensitively on the distribution of dislocations. For a crystal oriented for slip on a single family of slip planes, the dislocations move on parallel slip planes when the initial yield stress is exceeded. Under such conditions only slight work-hardening occurs, as shown by the easy-glide region or Stage I in the typical stress/strain curve for a f.c.c. single crystal (Fig. 41). The extent of Stage I is small and $\gamma \sim 0.01\text{-}0.1$ depending on orientation, temperature, and purity of the specimen; in close-packed hexagonal crystals, however, in which slip occurs mainly on basal planes, easy glide is much more extensive. In easy glide the dislocations mostly glide out of the crystal at the free surface, as indicated by the slip-line pattern which is of fine slip with very long slip lines comparable with the diameter of the specimen. This stage is terminated because of the occurrence of small amounts of slip on secondary systems intersecting the primary glide planes; these dislocations are called forest dislocations. The secondary slip may be activated by the stress concentrations produced where primary glide dislocations have piled-up against previously stopped dislocations, impurity particles, and even the oxide film on the surface, or because the crystal rotation relative to the stress axis that takes

place during deformation brings a second slip system into a favourable orientation. Crystals oriented to glide on two slip systems (Fig.42) from the start, usually begin plastic deformation with stage II, omitting stage I completely. Whatever the reason, this turbulent, rather than laminar flow, of dislocations leads to a stage of strong work-hardening, indicated in Fig. 41 as stage II. The work-hardening rate in this stage, also called the linear-hardening region, is $d\tau/d\gamma = \theta_{II} \sim 10^{-2}\mu$ and is approximately independent of temperature. Three-stage hardening is also observed in b.c.c. metals, but the work-hardening rate is a little less than in f.c.c. crystals, i.e. $\theta_{II} \sim \mu/500$. Several mechanisms for stage-II hardening have been proposed, in which the flow stress is controlled either by long-range stresses from piled-up groups of dislocations* or by interactions with forest dislocations* by sessile jogs on gliding dislocations,+ or by bowing out of lengths of dislocation in the network.‡ The hardening rate depends on the arrangements of dislocations assumed. At present, detailed electron microscopical observations on the nature of the dislocation structure in deformed crystals are available only for copper, but general observations on other f.c.c. crystals and some b.c.c. crystals have revealed dipoles, tangles, and cell structures similar to those found in copper.** Work-hardening models based on a non-uniform distribution of dislocations alone are applicable and that proposed by Hirsch++ following an electron-microscope study of copper, is outlined here.

Electron microscopical observations show that in stage I bands of dipoles are formed (Fig. 43) elongated normal to the primary Burgers vector direction. Their formation is associated with isolated forest dislocations and individual dipoles are~1 μm in length and a few hundred Angstroms wide. Different patches are arranged at spacings of~10 μm along the line of intersection of a

A Seeger, "Dislocations and Mechanical Properties of Crystals", p.243, 1957: New York and London (John Wiley).

**Z.S. Basinski, Phil. Mag. 1959, 4, 383.*

+*P.B. Hirsch, ibid, 1962, 7, 67, See also N.F. Mott, Trans. Met. Soc. A.I.M.E. 1960, 218, 962.*

‡*D. Kuhlmann-Wilsdorf, Trans. Met. Soc. A.I.M.E. 1962, 224, 1047.*

***P.B. Hirsch and J. Steeds. "The Relation between Structure and Mechanical Properties of Metals", Vol. I, p.39. 1963: London (H.M. Stationery Office).*

++*P.B. Hirsch, ibid., p.48.*

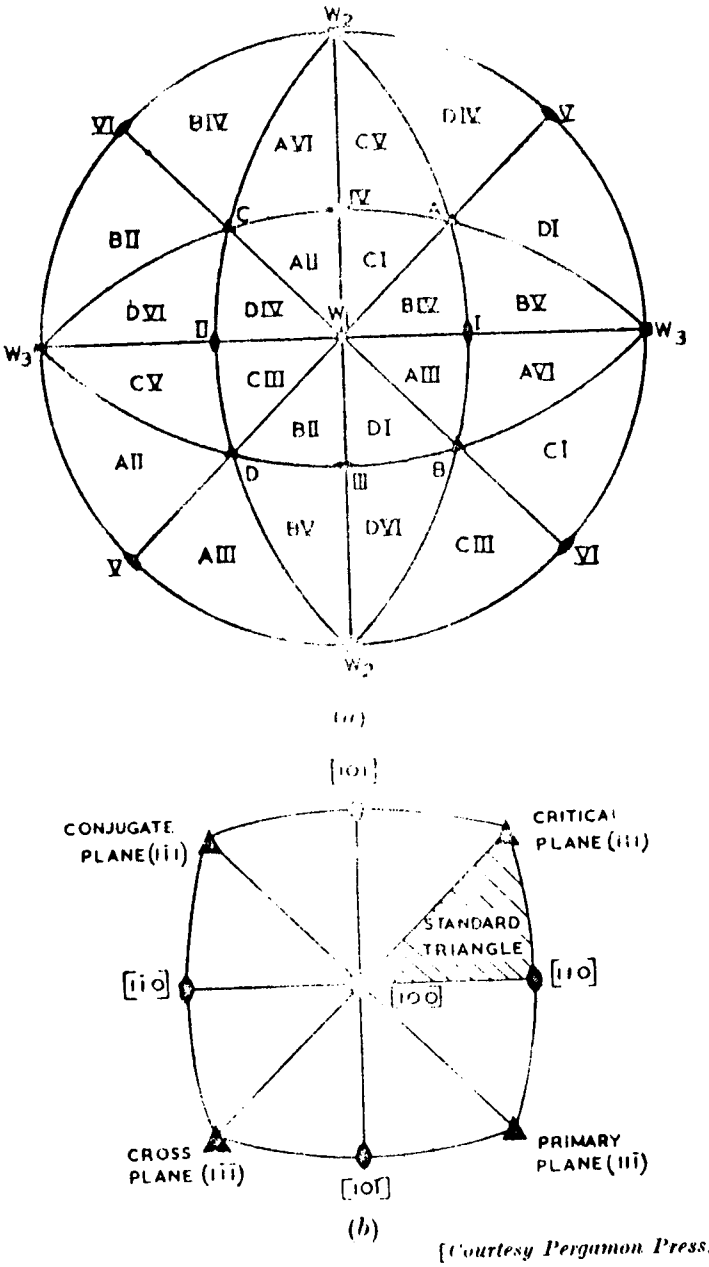

Courtesy Pergamon Press.

Fig. 42. Stereographic projections of: (*a*) slip planes A–D and directions (*b*) terminology of slip planes. (*After Clarebrough and Hargreaves.*)

secondary slip plane with the primary slip plane. With increasing strain in stage I the size of the gaps between the dipole clusters decreases and therefore the stress required to push dislocations through these gaps increases.

The room temperature work-hardening rate in stage I is $\sim \mu/5000$ in f.c.c. and $\mu/10,000$ in b.c.c. crystals. Stage II begins (Fig. 43) when the applied stress plus internal stress resolved on the secondary systems is sufficient to activate secondary sources near the dipole clusters. The resulting local secondary slip leads to local interactions between primary and secondary dislocations both in the gaps and in the clusters of dipoles, the gaps being filled with secondary dislocations and short lengths of other dislocations created by interactions, e.g. Lomer-Cottrell dislocations in f.c.c. crystals and $a\langle 100\rangle$ -type dislocations in b.c.c. crystals. Dislocation barriers are thus formed surrounding the original sources.

In stage II (Fig. 43) it is proposed in the model that dislocations are stopped by elastic interaction when they pass too close to an existing tangled region with high dislocation density. The long-range internal stresses due to the dislocations piling up behind are partially relieved by secondary slip, which transforms the discrete pile-up into a region of high dislocation density containing secondary dislocation networks and dipoles. These regions of high dislocation density act as new obstacles to dislocation glide, and since every new obstacle is formed near one produced at a lower strain, two-dimensional dislocation structures are built-up forming walls of an irregular cell structure. With increasing strain the number of obstacles increases, the distance a dislocation glides decreases, and therefore the slip-line decreases in stage II; slip-line metallography indicates that the length L of slip lines in stage II varies according to the relation $L = \Lambda/(\gamma-\gamma^*)$ where γ^* is the strain at the onset of stage II and Λ is a constant $\sim 10^{-4}$ cm. In this model, the work-hardening rate depends mainly on the effective radius of the obstacles, considered to be a constant fraction k of the discrete pile-up length on the primary slip system, and is given by $\theta_{II} = k\mu/8\pi$ For a f.c.c. crystal with orientation in the centre of the stereographic unit triangle $k \simeq 1/12$ and $\theta_{II} \simeq \mu/300$.

The onset of stage III, or parabolic, hardening is strongly temperature-dependent and metallography shows that the length of the slip lines increases substantially, the slip lines being interconnected with short cross-slip lines. The work-hardening rate is lower than in stage II, mainly because screw

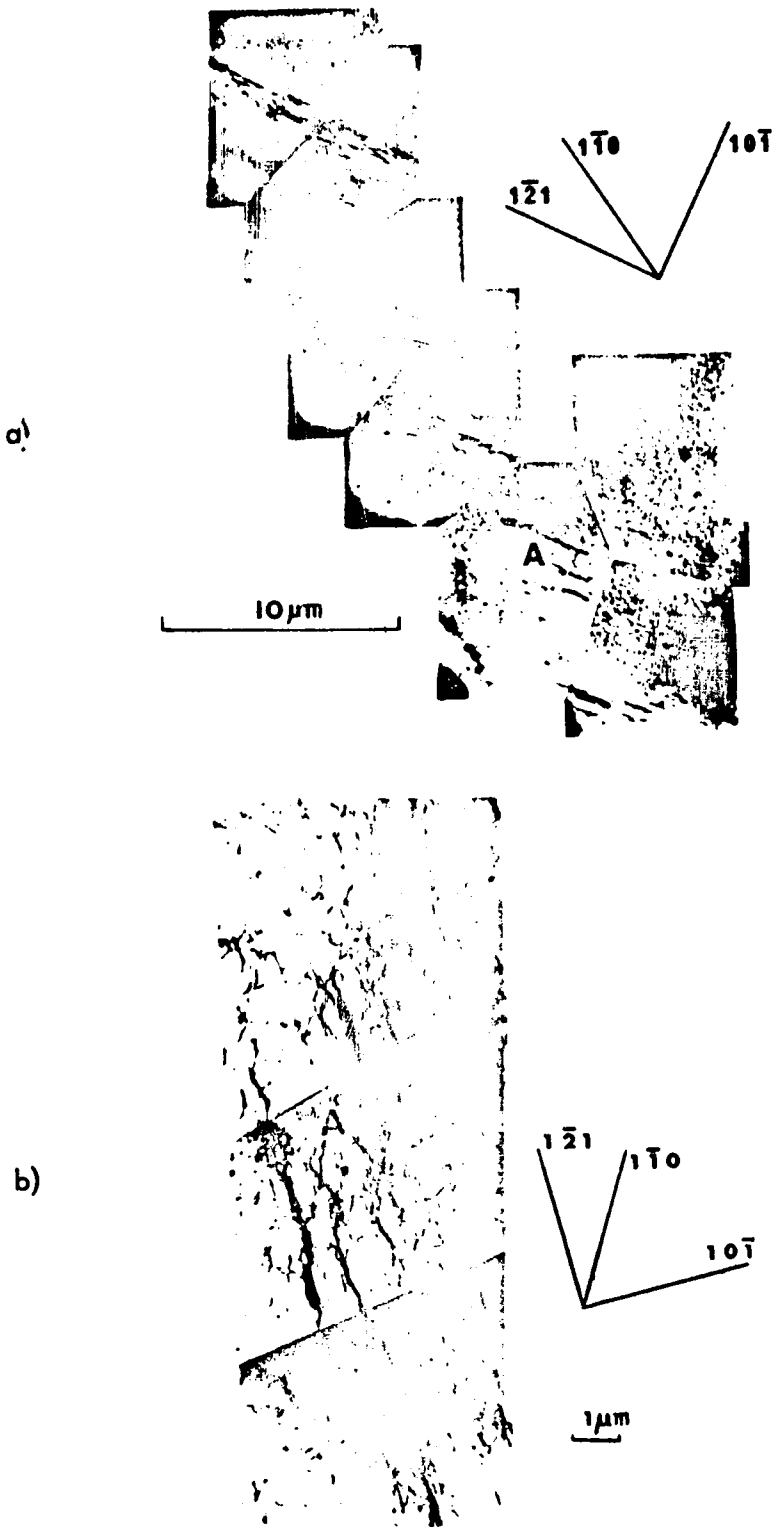

Fig. 43.

Dislocation structure in deformed copper single crystal: a) in Stage I; b) at the beginning of Stage II; c) at the end of Stage II; d) in Stage III. (After Steeds.)

dislocations can cross-slip and so by-pass the obstacles that hindered dislocation motion in the previous stage. Electron-metallographic observations on sections of deformed crystal inclined to the slip plane Fig. 43 (d) show the formation of a cell structure in the form of boundaries, approximately parallel to the primary slip plane of spacing $\sim 1 - 3 \mu m$, plus other boundaries extending normal to the slip plane as a result of cross-slip.

Polycrystals.

Metals normally used contain a large number of randomly oriented grains, or crystals, separated by grain boundaries. Field-ion microscopical observations show that these boundaries are only ~ 2 atoms thick; across them the atoms are disordered and transfer their allegiance from the one crystal to the other. The boundary may be considered as a surface containing an array of dislocations, these arrays having a simple structure in the case of low-angle boundaries and a more complex structure in the case of the more usual high-angle boundaries, where the dislocations are so close together that it is difficult to distinguish one from another.

At intermediate and low temperatures, polycrystalline metals deform plastically by slip within the individual grains; each grain remaining joined to its neighbours in such a way that it deforms to a shape dictated by them and in conformity with that of the specimen as a whole. To achieve this it is necessary for glide to occur simultaneously on several differently oriented slip systems; the crystal must glide on at least five geometrically independent slip systems, although if extensive cross-slip is available the operation of three non-coplanar, non-orthogonal slip directions can produce an arbitrary strain. In metals with f.c.c. structure there are two independent shear systems in each slip plane, giving a total of eight; and in b.c.c. metals the number is even greater. These metals therefore have sufficient glide systems for polycrystalline ductility. By contrast, metals with non-cubic structure, intermetallics and ceramics are often hard and brittle in polycrystalline form because each grain normally deforms by glide on less than the required number of systems; hence to achieve the necessary general plasticity additional "hard" slip systems have to

operate, e.g. non-basal slip or twinning in hexagonal metals. Fortunately, these hard glide systems often show a strong temperature-dependence, probably due to the Peierls stress, which enables such materials to be plastically deformed at high temperatures, i.e. hot worked.

The importance of grain boundaries as a source of strengthening is indicated by the increased yield and flow stress of polycrystals compared with single crystals. In fact, many materials are observed to obey the Petch relationship.

$$\sigma = \sigma_0 + kd^{-\frac{1}{2}} \qquad 25.$$

where σ is the tensile flow stress for a given strain d is the average grain diameter, σ_0 is interpreted as a friction stress resisting dislocation motion, and k is a constant. This relationship can be explained by considering the difference between slip in a single crystal and in a polycrystal.

When axial tensile stress σ is applied to a single crystal, the shear stress produced on the most favourably oriented slip plane is $\tau = \sigma/m$, where m is an orientation factor with a minimum value of 2. If a polycrystal behaves simply as a collection of randomly oriented free crystals then the tensile flow stress would be given by a relation $\sigma = m\tau$, with an average value for m which Sachs* calculated for f.c.c. structures to be 2.2. This simple behaviour is not possible, however because of the need to maintain continuity between grains; this leads to deformation on less favourably oriented grains and an m value greater than the Sachs value and equal to 3.1 according to Taylor.+

Such a treatment takes no account of grain size and this must be considered because dislocations arriving at a free surface in a single crystal

*G. Sachs, Z.v.d.I. 1928, 72, 734.

+G.I. Taylor, J. Inst. Metals, 1938, 62, 307.

can emerge, whereas in a polycrystal the dislocations cannot freely cross a grain boundary (Fig. 44). Armstrong et al* have considered this problem and their treatment is largely followed here. If τ_0 is the stress a slip band could sustain if there were no resistance to slip across the grain boundary, i.e. a friction stress approximately equal to the critical shear stress of a free single crystal, and τ is the higher stress sustained by a slip band in a polycrystal, then $(\tau - \tau_0)$ represents the resistance offered by the boundary, which reache a limiting value when slip is induced across the boundary in the next grain. The influence of grain size can be explained if the length of the slip band is proportional to d. Thus, since the stress concentration at a short distance r from the end of the slip band is proportional to $(d/4r)^{\frac{1}{2}}$, the maximum shear stress at a distance r ahead of a slip band carrying

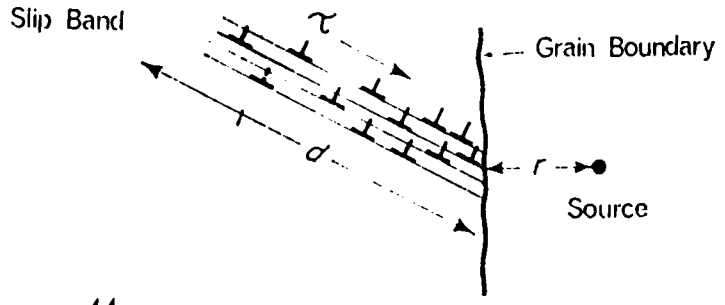

Fig. 44. Grain-boundary blocking of a slip band.

an applied stress τ in a polycrystal is given by $(\tau - \tau_0)\left[d/4r\right]^{\frac{1}{2}}$ and lies in the plane of the slip band. If this maximum stress has to reach a value τ_{max} to operate a new source at a distance r, then

*R. Armstrong, I. Codd, R.M. Douthwaite and N.J. Petch, Phil. Mag. 1962, 7, 45.

$$(\tau - \tau_0) \left[d/4r\right]^{\frac{1}{2}} = \tau_{max}$$

or rearranging

$$\tau = \tau_0 + (\tau_{max} 2r^{\frac{1}{2}}) d^{-\frac{1}{2}}$$

which may be written as

$$\tau = \tau_0 + k_s d^{-\frac{1}{2}} \qquad 26.$$

It then follows that the tensile flow curve of a polycrystal is given by

$$\sigma = m(\tau_0 + k_s d^{-\frac{1}{2}}) \qquad 27.$$

and hence, from the Petch equation

$$\sigma_0 = m\tau_0 \quad \text{and} \quad k = mk_s$$

Now, just as there is an orientation factor on a macroscopic scale in developing the critical shear stress within the various grains of a polycrystal so there is a local orientation factor in operating a dislocation source ahead of a blocked slip band. The slip plane of the source will not, in general, lie in the plane of maximum shear stress, and hence τ_{max} will need to be such that the shear stress τ_σ required to operate the new source must be generated in the slip plane of the source. In general, the orientation factor dealing with the orientation relationship of adjacent grains will be different from that arising from the macroscopic effects of slip-plane orientation relative to the axis of stress, so that $\tau_{max} = \frac{1}{2}m'\sigma$. For simplicity Armstrong et al assumed $m' = m$ and hence the parameter k in the Petch equation is given by $k = m^2 \tau_\sigma r^{\frac{1}{2}}$.

It is clear from the above treatment that the parameter k depends essentially on two main factors. The first is the stress to operate a source dislocation, and this depends on the extent to which the dislocations

are locked by impurity atoms or point defects. Strong locking implies a large unpinning stress and hence a large k. The reverse is true for weak locking. The second factor is contained in the parameter m which depends on the number of available slip systems. A multiplicity of slip systems enhances the possibility for plastic deformation and so implies a small k. A limited number of slip systems available would imply a large value of k. It then follows that; (i) for f.c.c. metals k will generally be small, i.e. there s only a small grain-size dependence of the flow stress, (ii) for h.c.p. metals k will be large because of the limited slip systems, and (iii) for b.c.c. metals k will be large because of the strong locking. Of particular importance in b.c.c. metals is the variation with grain size of the lower yield tensile stress σy i.e. the stress to propagate a Luders band (Fig.38) in a tensile specimen. This is usually expressed as

$$\sigma y = \sigma_0 + kyd^{-\frac{1}{2}}$$

where ky is the appropriate value of k $(=\sigma_c r^{\frac{1}{2}})$.

On this theory, the term ky is a measure of the stress to unlock a dislocation from its atmospheres and, since the binding of a solute atom to a dislocation is short-range in nature and hence effective only over an atomic distance or so, should depend sensitively on temperature. A linear relation between the lower yield stress, σy , and the reciprocal of the square root of the grain size is observed for all the refractory metals with b.c.c. structure. However, ky is found to be dependent on temperature only in the early stages of ageing, as for example, after quenching* or on re-ageing following over-straining+ With continued ageing ky becomes temperature-independent, as shown in Fig. 45 . The interpretation of ky therefore depends on the degree of strain-ageing. In lightly aged iron the dislocations are weakly locked by solute atoms and the yield process takes place by unpinning the dislocations from their impurity atmospheres. Under these conditions ky is strongly dependent on temperature. In general, however, the dislocations in well-annealed iron are strongly locked by impurities, and

*R.M. Fisher and A.H. Cottrell, "The Relation between Structure and Mechanical Properties", Vol. II, p.455. 1963: London (H.M.S.O.).

+T.C. Lindley and R.E. Smallman, Acta Met., 1963, 11, 361.

sometimes take the form of definite precipitates. Under these conditions the yielding can propagate from grain to grain either; (i) by pulling away from the anchoring points if the precipitates are sufficiently coarsely spaced, or (ii) by creating dislocations at a grain boundary where the stress concentration resulting from the slip band is highest, rather than unpinning dislocations inside the grains. Both these processes are relatively insensitive to temperature so that a temperature-independent k_y will be obtained, as observed. The strong temperature-dependence of the yield stress then arises from the σ_0 term contributed by precipitates and other dislocations, as well as the Peierls-Nabarro lattice stress.

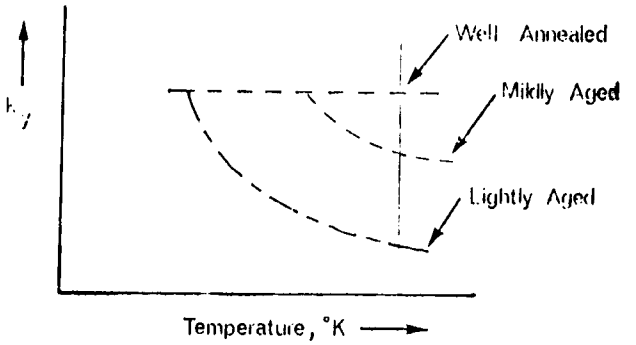

Fig. 45. Variation of k_y with temperature.

Once free dislocations are created, the yield-point phenomenon is accentuated by the rapid increase in dislocations by the cross-glide multiplication process. The sharp yield phenomenon may therefore be represented in the following manner. As the specimen is loaded up to the lower yield stress the number of mobile dislocations is zero at σ_0, the stress to cause dislocation motion. At some higher stress a few dislocations are released athermally either from grain boundaries or from the precipitates that anchor them, at regions of high stress concentration. The velocity of

dislocation depends sensitively on stress, and hence with further increase in stress some dislocation multiplication occurs; this stage would correspond to the pre-yield micro-strain often observed in these metals. The number of dislocations participating is small, so that plastic flow is limited and, since the tensile machine cross-head is moving at a constant rate, the stress increases to a value where the dislocation velocity becomes quite high. At a critical stress, corresponding to the upper yield stress, sudden intense multiplication occurs, because of the high stress value. However, the dislocation density is related to the strain rate by an equation of the form $\dot{\epsilon} = \rho b v$, where v is the dislocation velocity, so that the product ρv becomes greater than that needed to deform the crystal at the applied strain rate. Thus a lower average velocity of dislocations is required to maintain a constant strain rate, and as the change in stress for a given change in velocity is large, a substantial yield drop results.

In this alternative model of yielding, impurity atoms are still necessary for the occurrence of the yield point, since by causing the initial distribution of dislocations to be locked, the number of dislocations that can contribute to the deformation process at the stress σ_0 i.e. the stress needed to move fresh or unlocked dislocations at a reasonable velocity, is limited. Locking, however, is not the only requirement, as both rapid multiplication of dislocations and a large dependence of dislocation velocity on stress are also necessary for prominent yield drop. In over-aged material, the dislocations are all essentially unlocked and on reloading the sample many free dislocations can participate in the initial deformation. Consequently, the stress - and hence the dislocation velocity - does not reach a high value; the transition from the elastic to the plastic state is, therefore, more gradual. During strain-ageing the impurity atoms diffuse to free dislocations, relocking them by forming Cottrell atmospheres following light ageing, or precipitates after extensive ageing; the stage is then reset for a new yield phenomenon.